Organic & Biomolecular Chemistry

PAPER

View Article Online
View Journal

Cite this: DOI: 10.1039/c4ob01339e

Synthesis of tumor-associated MUC1-glycopeptides and their multivalent presentation by functionalized gold colloids†

Isabella Tavernaro,‡[a] Sebastian Hartmann,‡[b] Laura Sommer,[c] Heike Hausmann,[d] Christian Rohner,[a] Martin Ruehl,[c] Anja Hoffmann-Roeder[e] and Sabine Schlecht*[a]

Received 27th June 2014,
Accepted 29th July 2014

DOI: 10.1039/c4ob01339e

www.rsc.org/obc

The mucin MUC1 is a glycoprotein involved in fundamental biological processes, which can be found over-expressed and with a distinctly altered glycan pattern on epithelial tumor cells; thus it is a promising target structure in the quest for effective carbohydrate-based cancer vaccines and immunotherapeutics. Natural glycopeptide antigens indicate only a low immunogenicity and a T-cell independent immune response; however, this major drawback can be overcome by coupling of glycopeptide antigens multivalently to immunostimulating carrier platforms. In particular, gold nanoparticles are well suited as templates for the multivalent presentation of glycopeptide antigens, due to their remarkably high surface-to-volume ratio in combination with their high biostability. In this work the synthesis of novel MUC1-glycopeptide antigens and their coupling to gold nanoparticles of different sizes are presented. In addition, the development of a new dot-blot immunoassay to test the potential antigen–antibody binding is introduced.

Introduction

Immunotherapy, a potential alternative to the established cancer therapy, is based on the possibility of activating the human immune system to recognize and effectively kill tumor cells.[1,2] In comparison with standard cancer therapies, such as surgical removal of tumors, radiation and chemotherapy, this approach has the advantage of high selectivity and the delocalization of the immune reaction.[3] With the help of synthetic vaccines the immune system would not only be activated to attack malignant cells specifically with minimal detriment to healthy cells, but also provide an opportunity to target primary and secondary metastases for the first time. Furthermore, an immunological memory that would provide long-term protection against new cancer diseases could be possible.[4] In contrast to bacteria, viruses or other pathogens, tumor cells are endogenous materials against which the immune system necessarily shows tolerance. Therefore the synthetic vaccines also need to trigger a specific immune response, leading to the formation of antibodies that differentiate between normal and cancer cells.

To distinguish between healthy and tumor cells, cell surface glycoproteins have proven to be potential target structures.[5] These so-called mucins[6] are a heterogeneous family of large and high molecular weight *O*-glycoproteins; the most studied member is the membrane-bound glycoprotein MUC1, found ubiquitously on the apical surface of epithelia and consists of numerous 20-mer-tandem repeats of the sequence HGVTSAPDTRPAPGSTAPPA which embodies five potential glycosylation sites.[7] However, due to variations in enzyme activities, which lead to altered glycosylation patterns, these surface glycoproteins are modified on epithelial tumour cells. For example, MUC1 is overexpressed, distributed over the entire cell surface and bears smaller less branched tumor-associated carbohydrate antigens (TACA) in its tumor-associated form.[8] Therefore, tandem repeat MUC1-glycopeptides with TACA side chains are of particular interest for antitumor vaccines.[9]

Although various mucin-type glycopeptides decorated with different TACA side chains have been successfully investigated

[a]*Institute of Inorganic and Analytical Chemistry, Justus-Liebig-University Giessen, Heinrich-Buff-Ring 58, 35392 Giessen, Germany. E-mail: Sabine.Schlecht@anorg.chemie.uni-giessen.de*
[b]*Institute of Organic Chemistry, Johannes Gutenberg-University Mainz, Duesbergweg 10-14, 55128 Mainz, Germany*
[c]*Institute of Food Chemistry and Food Biotechnology, Justus-Liebig-University Giessen, Heinrich-Buff-Ring 58, 35392 Giessen, Germany*
[d]*Institute of Organic Chemistry, Justus-Liebig-University Giessen, Heinrich-Buff-Ring 58, 35392 Giessen, Germany*
[e]*Institute of Organic Chemistry, Ludwig-Maximilian-University Munich, Butenandtstr. 5-13, Haus F, 81377 Munich, Germany*
†Electronic supplementary information (ESI) available. See DOI: 10.1039/c4ob01339e
‡These authors contributed equally to this work.

as molecularly defined vaccine prototypes for triggering strong humoral immunity over the last few years,[10] their targeting is often constricted by a limited metabolic stability, a weak immunogenicity and a T-cell-independent immune reaction.[11] For that reason various strategies for vaccine design have focused on the enhancement of the immune response by the conjugation of TACAs and tumor-associated MUC1-glycopeptide fragments to immunogenic carriers like keyhole limpet hemocyanin, tetanus toxoid or BSA.[12] For example, synthetic vaccines composed of tumor-associated MUC1 sequences, T-cell epitopes and Toll-like receptor 2 (TLR2) ligands elicited a strong immune response.[13] Also, highly fluorinated MUC1-glycopeptide antigens have been developed.[14] Another promising approach to enhance antigen density and therefore to overcome the mentioned obstacles is a multivalent antigen presentation by different templates such as immunogenic peptides,[15] dendrimers,[16] liposomes[17] or bioactive nanoparticles.[18] Although still at the beginning of its development, the first successful results indicate the great potential of MUC1-functionalized nanoparticles. The concept of multivalency describes the chemical interaction of multiple ligands of a biological unit with multiple receptors of another.[19] The resulting bonds are, in many cases, significantly stronger than the mere multiplication of the individual amounts. In previous work we could indicate that the multivalent presentation of potential binding epitopes on the surface of nanoparticles can lead to higher binding affinities[20] and so it is interesting to investigate their possible use in anti-cancer vaccines presentation.[21] Recently, for example, the synthesis of nanosized polymer-based glycopeptide vaccines, which induce significant immune reactions in mice, was described.[22] Due to their lack of immunogenicity, their remarkably high surface-to-volume ratio in combination with their high stability, and low toxicity[23] gold nanoparticles are also well suited as templates for the multivalent presentation of antigens.

Herein, we present the synthesis and immobilization of novel MUC1-glycopeptide antigens by functionalized gold colloids and the detection of their selectively antigen–antibody binding by quartz crystal microbalance and a novel dot-blot immunoassay for the first time.

Results and discussion

Synthesis of the MUC1 glycopeptide antigen analogues

Following known strategies in the literature, the required building blocks such as the T_N-antigen **5** and the spacer **10** for the synthesis of glycopeptides were prepared individually in multi-step procedures and then assembled using solid-phase peptide synthesis.[24]

The synthesis of the T_N-antigen block **5** was carried out by a previously prepared *N*-acetylgalactosamine–threonine conjugate,[25] which reacted with a glycosyl donor through a variation of the Koenigs–Knorr glycosylation (Scheme 1a).[26] Then the *N*-acetylgalactosamine–threonine conjugate **4** was produced by the conversion of the azide function into an acetamido group through reductive acetylation.[27] In the terminal step the C-terminal *tert*-butylester protecting group was removed to achieve the desired glycosyl-aminoacid building block **5**. The spacer **10** is used to guarantee flexibility and distance between the nanoparticle and glycopeptide and because it can be easily coupled to the N-terminal amino acid of the peptide chain. Because of its primary amino function the spacer also allows another easy access to the coupling to the nanoparticles. The synthesis of the spacer **10** follows the method described by Keil *et al.*[16] (shown in Scheme 1b) and is described in detail in the Experimental section. The MUC1-glycopeptide antigens were assembled in an automated synthesizer by solid-phase peptide synthesis (SPPS) Fmoc-protocol employing trityl-TentaGel resin preloaded with Fmoc-Pro-OH, as previously described[24] (Scheme 1c). Low loaded resins were used to avoid interfering interactions of the growing peptide chain and all the functional groups of the amino acid side chains were protected by acid-labile protecting groups.

The coupling of the protected amino acids was performed with HBTU/HOBt and diisopropylethylamine (DIPEA) in DMF, while the coupling of the T_N-antigen block **5** was performed using the more reactive HATU/HOAt mix and *N*-methyl-morpholine (NMM) in *N*-methyl-pyrrolidine (NMP). The last step of the solid-phase synthesis was the attachment of the synthesized triethylene glycol spacer **10**, followed by the release of the glycopeptide **11** from the resin with simultaneous cleavage of the side chain amino acid protecting groups using an acidic mix of TFA–triisopropylsilane (TIS)–H_2O (10 : 1 : 1). Finally the glycopeptides were deacetylated with NaOMe in MeOH at pH 10 under *Zemplén* conditions.

According to the described synthesis a short glycosylated sequence consisting of nine amino acids and the spacer was prepared initially **GP-01**. This compound was used to test the immobilization on the particle surface and the resulting multivalent effect. Finally, a single glycosylated MUC1 partial structure with a full, 20 amino acids containing TR domain and the spacer was made **GP-02** and used for binding studies of the functionalized Au-NPs (Fig. 1).

Preparation of surface-modified gold nanoparticles and the immobilization of the glycopeptides by peptide coupling reaction

For a multivalent presentation of the prepared potential MUC1-glycopeptide antigen analogues **GP-01** and **GP-02** the synthesis of nearly monodispersed nanoparticles is necessary. In this work we focused on gold nanoparticles, due to their mentioned unique properties.[23] The synthesis of gold nanoparticles is known in the literature[28] and based on the reduction of a gold salt in the presence of a stabilizer. By variation of the reaction conditions functionalized gold nanoparticles with a diameter less than 10 nm and a narrow size distribution were obtained. Although with a multidentate thiolinker, like for example the bidentate lipoic acid, functionalized gold nanoparticles are nearly resistant against ligand exchange reactions and have a considerably higher stability in water,[29] we decided to bind the MUC1-glycopeptide antigen

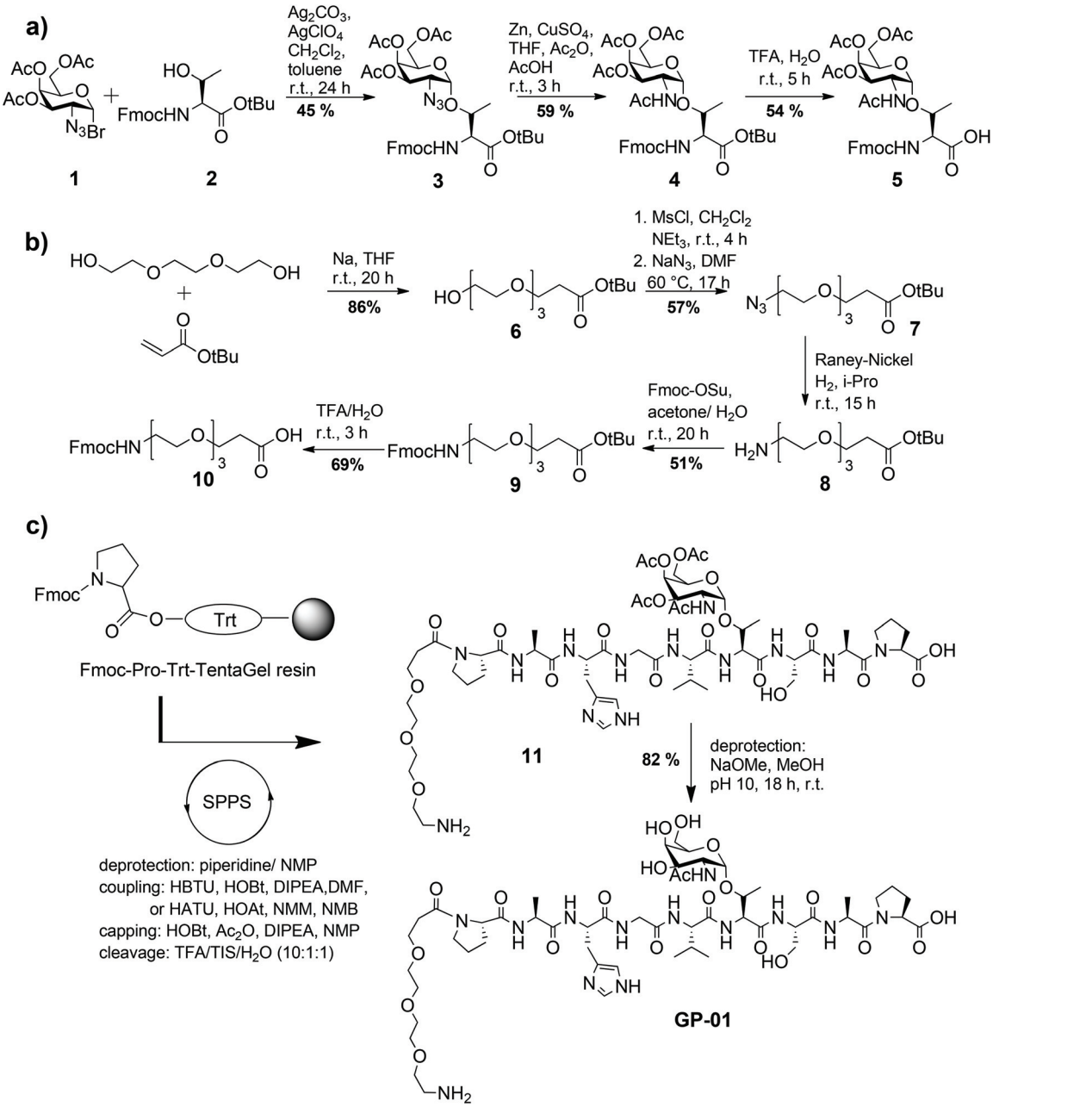

Scheme 1 Synthesis routes of the T_N-antigen (a) and the bi-functionalized triethylene glycol spacer (b). (c) Solid-phase peptide synthesis (SPPS) of the MUC1 like glycopeptides. Fmoc-Osu = *N*-(9*H*-Fluoren-9-ylmethoxycarbonyl)-succinimidylcarbonate NMP = *N*-methylpyrrolidone, HBTU = *O*-(1*H*-benzotriazole-1-yl)-*N*,*N*,*N*′,*N*′-tetramethyluronium hexafluorophosphate, HOBt = *N*-hydroxy-benzotriazole, DIPEA = diisopropylethylamine, HATU = *O*-(7-aza-benzotriazole-1-yl)-*N*,*N*,*N*′,*N*′-tetramethyl-uronium hexafluoro-phosphate, HOAt = *N*-hydroxy-7-azabenzotriazole, NMM = *N*-methylmorpholine, TIS = triisopropylsilane.

analogues covalently to the particle surface by a monodentate thiolinker based on 11-mercaptoundecanoic acid, which was used in our group previously.[20] Due to its limited required space on the particle surface the density of ligands should be higher.[30] The synthesis of *N*-hydroxysuccinimide-11-mercaptoundecanoate (MUDHSE) coordinated gold nanoparticles **14** with a diameter of 7 nm was carried out by a two-step route described in Scheme 2. In the first step dodecanethiol (DT) coordinated gold nanoparticles **12** were prepared by a one-pot synthesis, which was established by Stucky *et al.*[28] In the second step the dodecanethiol ligand was exchanged for the previously prepared *N*-hydroxysuccinimide-11-mercaptoundecanoate[24] **13** by a one step ligand exchange reaction in absolute DMF. To present the MUC1-glycopeptide antigen analogues multivalently, they were coupled to the prepared MUDHSE functionalized nanoparticles. Although the water solubility of the particles was a first hint of the successful immobilization, the characterization of the glycopeptide-func-

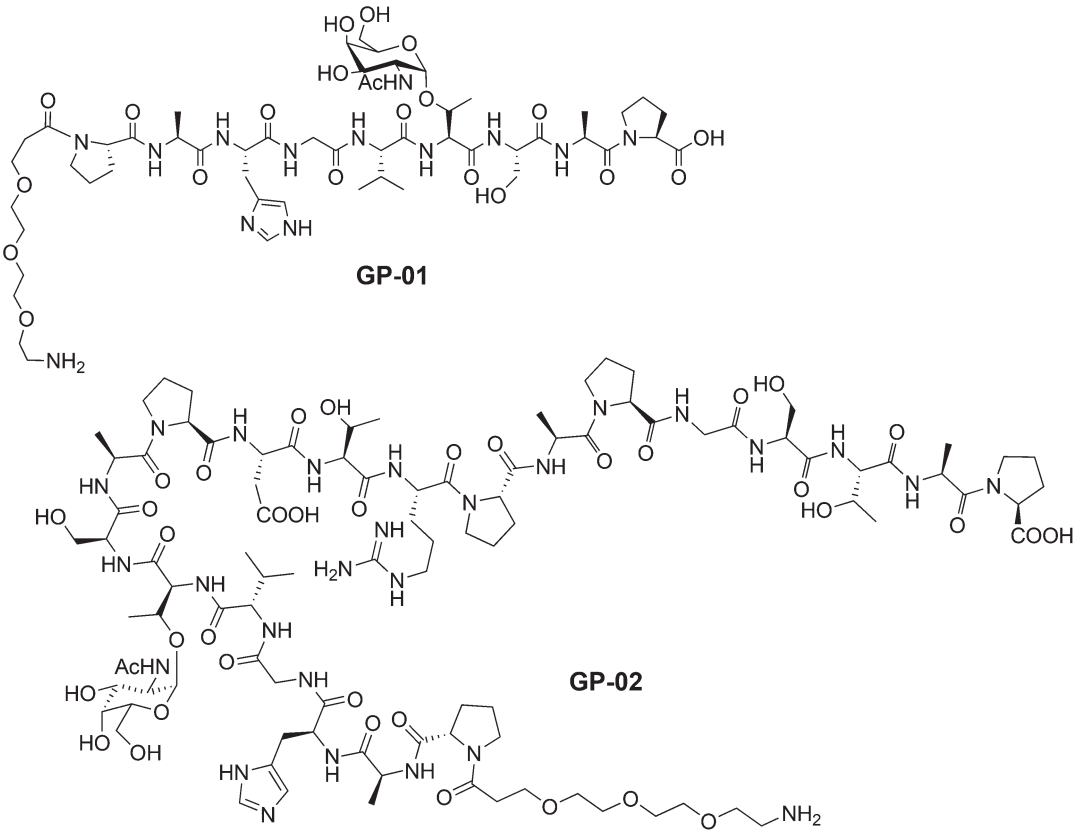

Fig. 1 Glycopeptides **GP-01** and **GP-02** with a PEG-spacer and a T_N antigen synthesized by SPPS.

tionalized nanoparticles was carried out by various methods. TEM images, UV/Vis spectra and dynamic light scattering (DLS) measurements were applied to determine the average diameter, shape and the size distribution of the nanoparticles. The TEM image shown in Fig. 2 indicates spherical particles with a narrow size distribution and an average diameter of 7 ± 1 nm. Also the UV/Vis spectra, which show only one maximum at 523 nm (Fig. 3), and the DLS measurements confirmed the total size including the shell of the particles with its adequate hydrodynamic diameter. In addition, the potential influence of the ligand exchange on the agglomeration state of the nanoparticles could be checked by these characterisation methods. There is no evidence that the ligand exchange reaction influences the agglomeration state. The successful change of the ligand shell was controlled directly by NMR spectroscopy. For this, the characteristic signals of the NMR spectra of the free glycopeptides were compared with those of the glycopeptide-coordinated gold nanoparticles. On the basis of 2D DQF-COSY and HSQC spectra, the newly formed amide bond could be clearly identified (Fig. 4 and 5). A differentiation between immobilized and free ligands is also possible through typical effects in nanoparticle NMR spectra. These effects are the significant line broadening and downfield shifts of the resonances of the immobilized ligands.[31] Unbound impurities and ligands retain their sharp resonances and can be distinguished from the bound ones. Moreover, IR spectra were used to prove the immobilization by identifying the amide bond.

Due to the fact that repulsive interactions of ligand molecules at less curved surfaces are weaker, a higher density of ligand molecules and thus a higher multivalent presentation could be possible on nanoparticles with a larger diameter.[23,32] To investigate this potential effect of the nanoparticle size on chemical and biological properties like stability, antigen presentation and bioavailability, we also synthesized and used gold nanoparticles with a larger diameter.

The large gold nanoparticles with a diameter of 14 nm were prepared by the well-known citrate method, which was first mentioned by Turkevich *et al.*[28b] The reaction is based on the reduction of the tetrachloroauric acid ($HAuCl_4$) with sodium citrate in water. Depending on the amount of citrate, it is possible to generate nanoparticles with a modest monodispersity and a size of around 10–20 nm. The citrate ligands of the large gold nanoparticles are only bound weakly *via* van der Waals interactions to the particle surface and so their replacement by water-soluble thiol-functionalized ligands is relatively facile. A ligand exchange with the *N*-hydroxysuccinimide-11-mercaptoundecanoate **13** is not realizable because of the insolubility of the active ester in water. For this reason, the coupling between the glycopeptides and the thiolinkers was carried out in the final step of the solid phase peptide synthesis. To avoid side reactions in the synthesis, the reactive thiol group had to

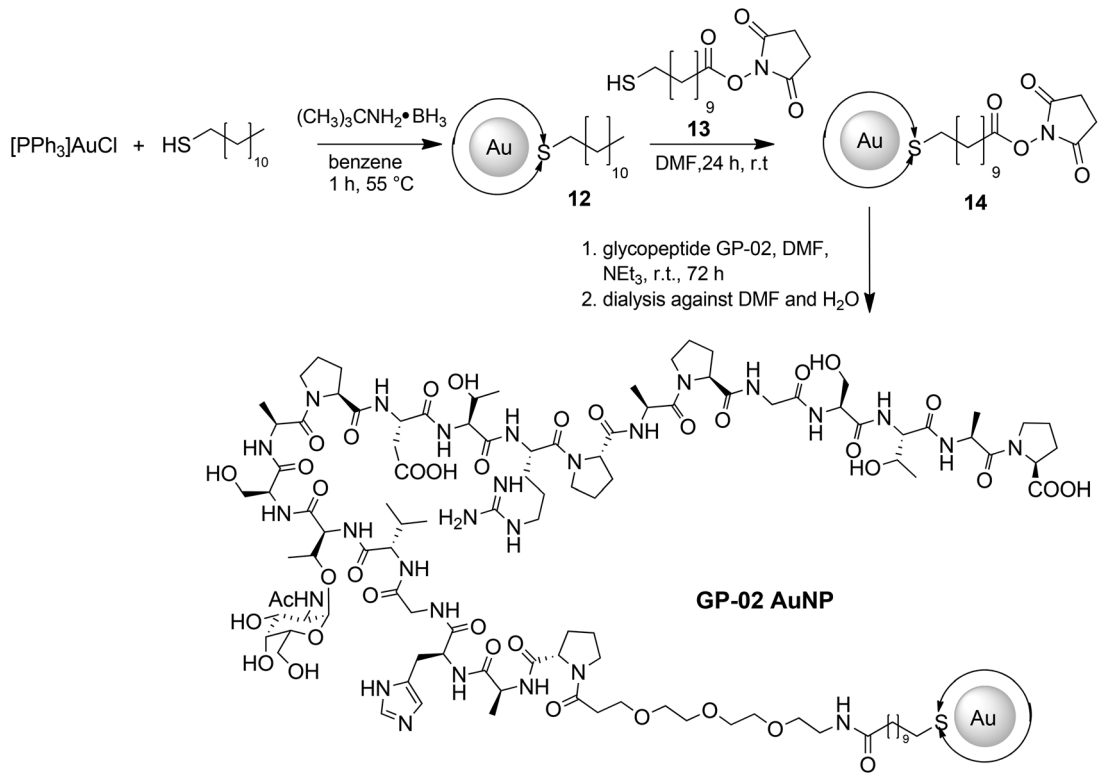

Scheme 2 Synthetic route for the preparation of nearly monodisperse gold nanoparticles with terminally functionalized thiol shell and the immobilization of the glycopeptide **GP-02** *via* postsynthetic shell modifications. Double arrows at the Au core represent the ligand shell completely surrounding the gold nanoparticles.

be protected, which was done by a trityl protecting group which could be removed like the other acid-labile side chain protecting groups during the cleavage from the resin. So, the linker **15** was prepared by the reaction of 11-mercaptoundecanoic acid with trityl chloride (Scheme 3a). After the solid phase peptide synthesis and the cleavage of the protecting groups the glycopeptide **GP-03** was immobilized by a ligand exchange reaction in water (Scheme 3b), followed by dialysis against water. The high affinity of the thiol linker to the gold nanoparticles and the resulting covalent bond lead to a full replacement of the citrate ligand.

The TEM images shown in Fig. 6 indicate that the received citrate coordinated gold nanoparticles have mostly a spherical shape, and only a small percentage of triangular nanoparticles deviate from it. The average diameter d = 14 ± 1 nm of the citrate coordinated gold nanoparticles was determined by TEM images and UV/Vis spectra. The hydrodynamic diameter received by DLS measurements is d_h = 18 ± 4 nm. The immobilization of the glycopeptides was checked by NMR and IR spectra. The aggregation state of the particles and the size and shape of the coordinated gold nanoparticles were also investigated like before by TEM, DLS measurements and absorption spectra. The obtained data indicated that the average diameter of the particle core remained 14 ± 1 nm and the maxima of the absorption spectra (Fig. 3) did not change (λ_{max} = 531 nm) either. This result confirms that the ligand exchange reaction had no effect on the particle and the agglomeration state.

Binding and immune tests of the glycopeptides coordinated gold nanoparticles

In order to investigate the biological activity of the glycopeptide nanoparticle conjugates, the **GP-02** coordinated AuNPs were tested in quartz crystal microbalance (QCM) experiments for their recognition by specific serum antibodies.[33] For that reason the commercially available anti-MUC1 antibody [SM3],[34] was used for detection of the antigen–antibody-binding. The QCM experiments were performed using commercially available quartz crystals coated with 100 nm gold layers. The binding of the SM3 antibody to the gold layer occurs through peripheral methionine binding sites, like Met18, Met34, Met82 and Met135[35] and because of this the methionine binding sites of the antibody do not interfere with the antigen binding site. During the QCM measurement the SM3 antibody was immobilized on the crystal, SM3 injection was stopped after no further increase in weight (Δf = const.) was achieved. After several washing steps with PBS buffer (Fig. 7), the **GP-02**-AuNP was added and washed again with PBS buffer.

After addition of the potential antigenic **GP-02** coordinated AuNP, a typical Langmuir adsorption isotherm was obtained. Due to the fact that the nanoparticle addition leads to a significant decrease of the Δf value, a binding of the GP-AuNP antigen colloids to the previously immobilized SM3 antibodies is indicated. At a certain point no further increase in weight

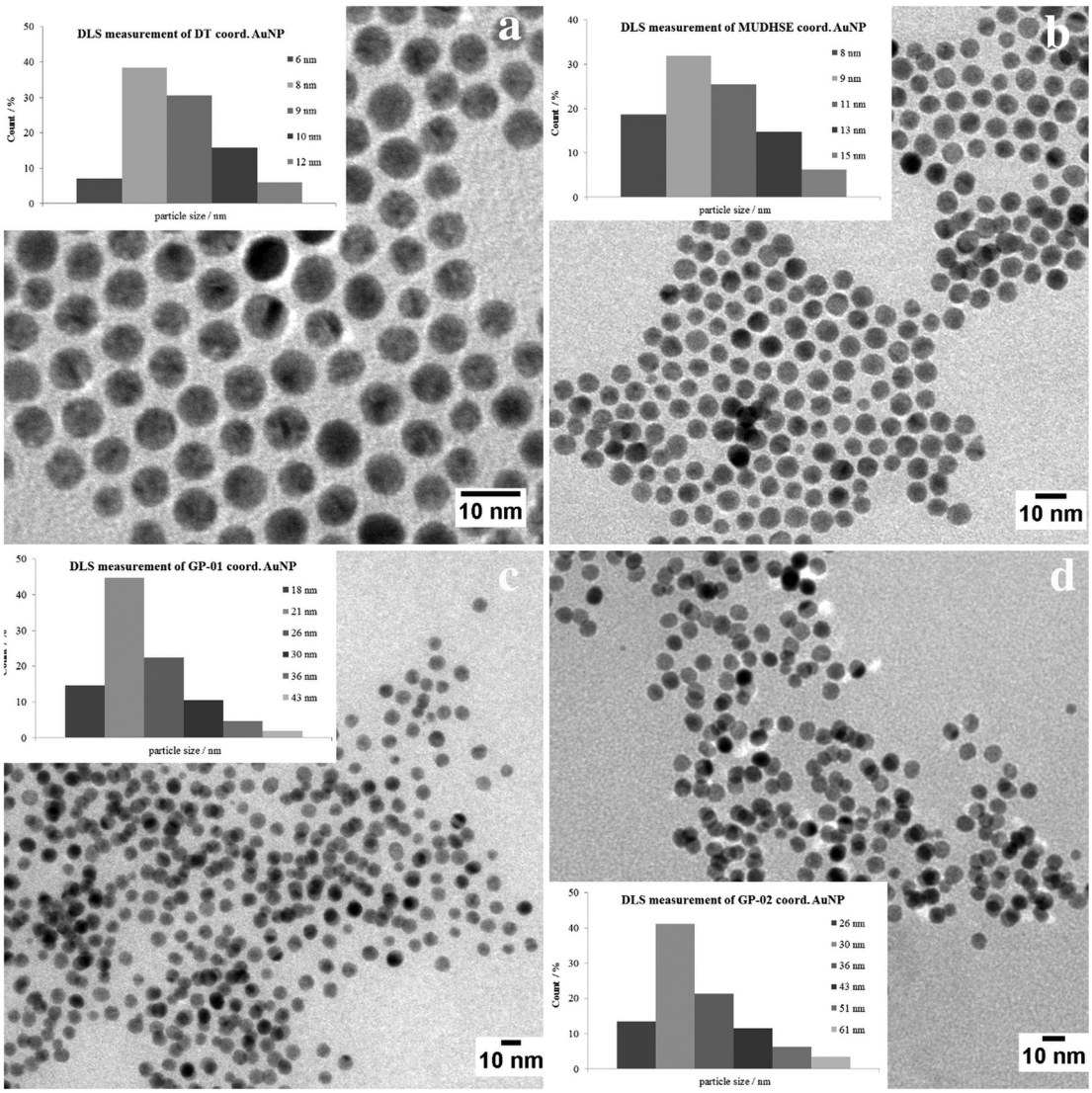

Fig. 2 TEM images of the synthesized gold nanoparticles with an average diameter of 7 nm. (a) DT coord. AuNP; (b) MUDHSE coord. AuNP; (c) **GP-01** coord. AuNP; (d) **GP-02** coord. AuNP.

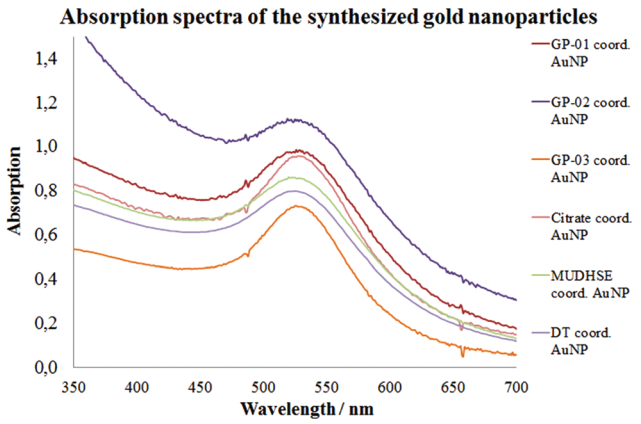

Fig. 3 UV/Vis spectra of the synthesized nanoparticles.

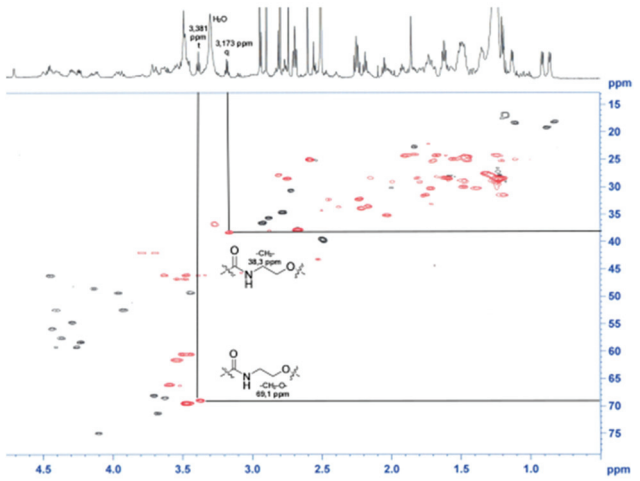

Fig. 4 HSQC-spectra of the **GP-01** coordinated AuNP; red = co-ordinated ligand, black = free glycopeptides.

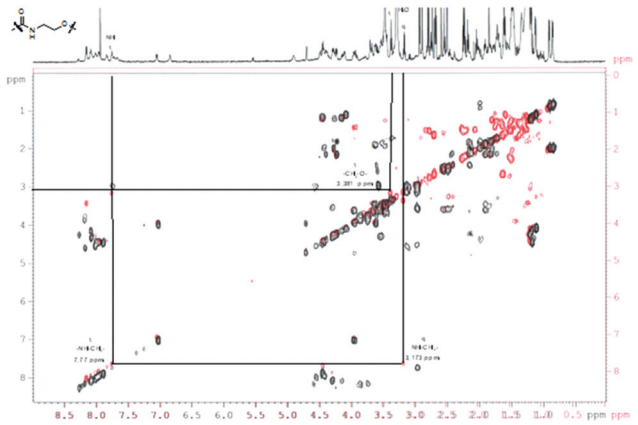

Fig. 5 COSY-DQF-spectrum of the **GP-01** coordinated AuNP; red = coordinated ligand, black = free ligand.

can be recognized; this is the point where all available antibodies are bound to the antigen coated nanoparticles.

The obtained result of the QCM experiment only indicates a binding of the GP-AuNPs to the SM3 antibody. To obtain information about the nature of the binding, the undiluted **GP-01** (c = 0.13 μM) and **GP-02** (0.32 μM) coordinated gold nanoparticle conjugates were tested in a simple and fast dot-blot immunoassay experiment. An undiluted citrate coordinated AuNP solution (c = 2.6 nM) was used as a negative control sample to preclude unspecific bindings of the gold particles. Also a serial dilution of **GP-02** coordinated AuNP was blotted to find the qualitative detection limits of the dot-blot immunoassay experiment.

The principle of the developed dot-blot immunoassay is shown in Fig. 8. Firstly the undiluted **GP-01** and **GP-02** coordinated AuNP, the serial dilution of **GP-02** coordinated AuNP and the negative control (AuCitrate) were immobilized onto the nitrocellulose membrane and incubated overnight (Fig. 9a). The colored dots of the undiluted gold nanoparticles were still visible after several washing steps with PBS, which indicates that the immobilization of the gold nanoparticles onto the nitrocellulose membrane was still intact. In the second step the membrane was blocked by milk powder in PBS buffer for 2 h at room temperature to block the remaining sites of the nitrocellulose membrane, and then the primary antibody (monoclonal anti-MUC1 antibody) was added and attached to the antigen. In the next step the enzyme-labeled

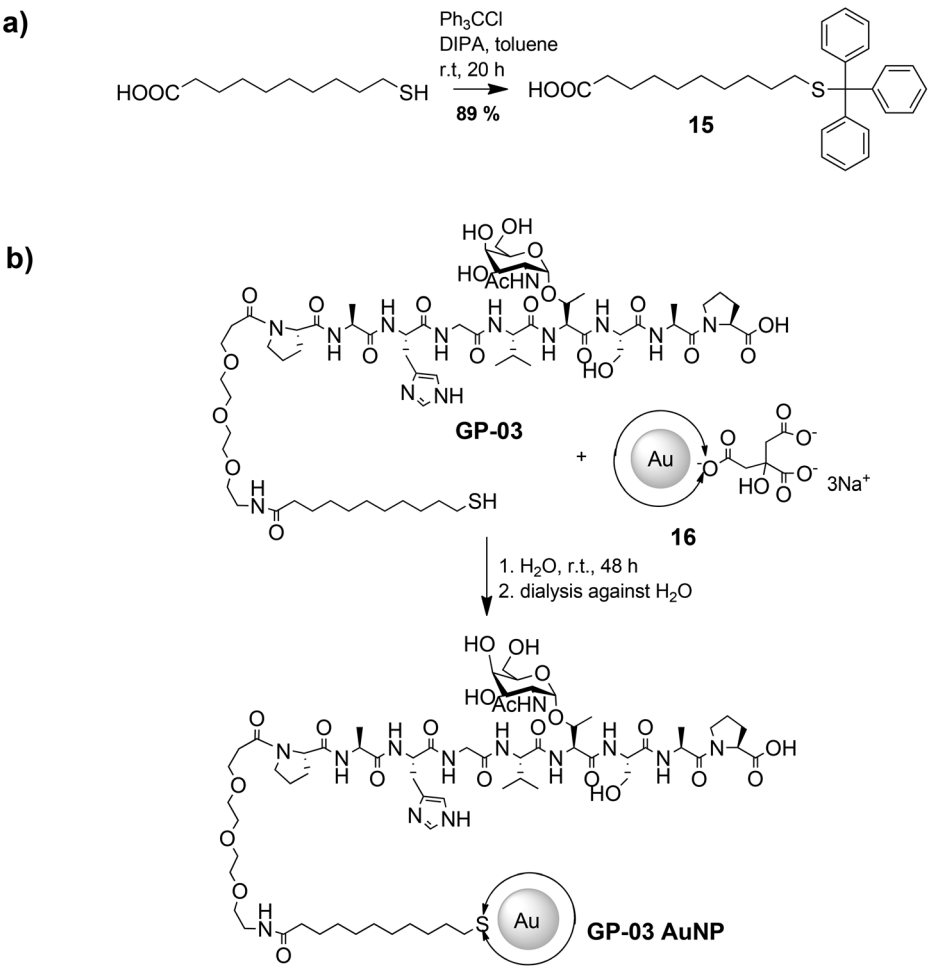

Scheme 3 Synthetic procedure of the immobilization of glycopeptides on the surface of large gold nanoparticles.

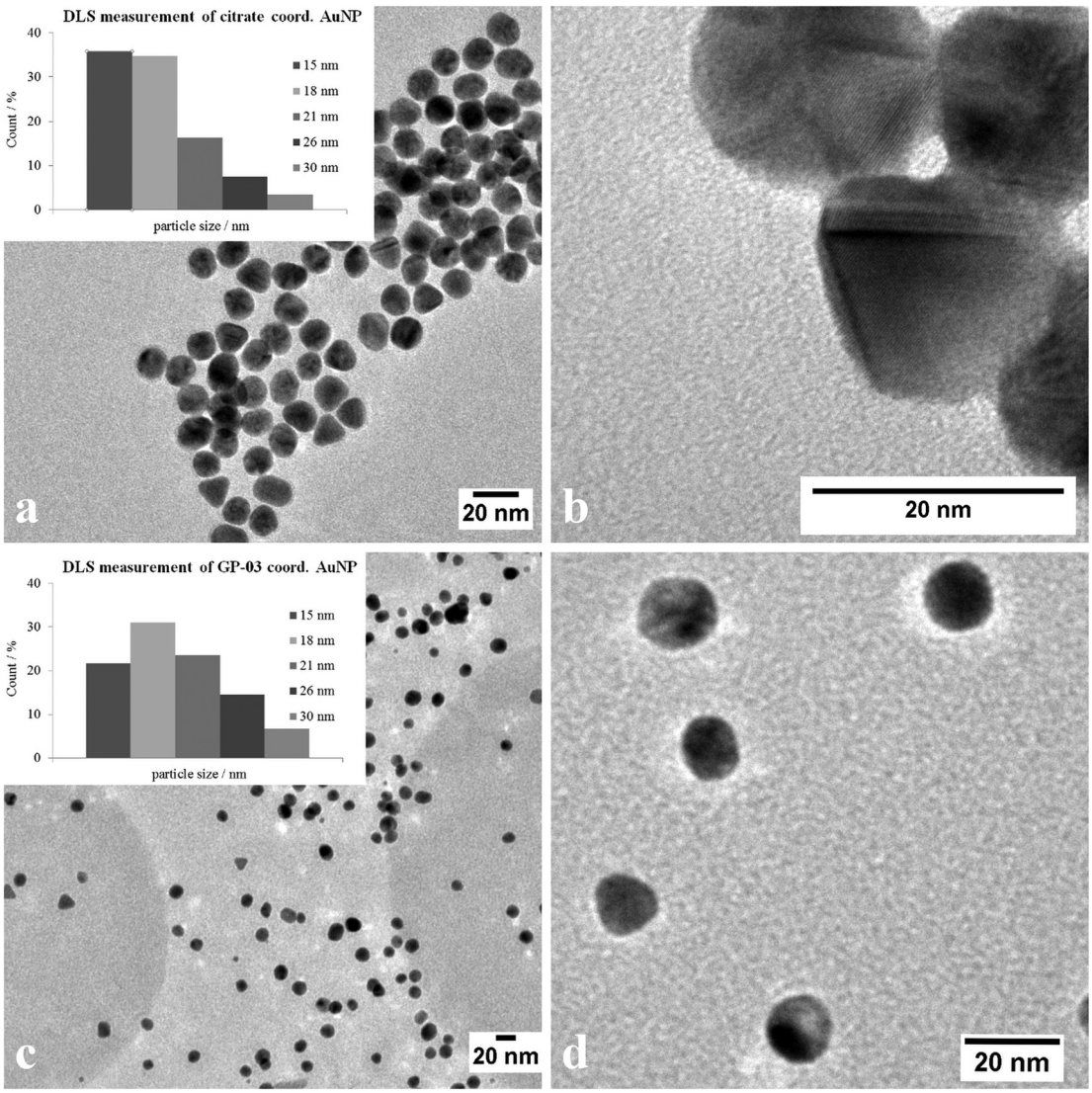

Fig. 6 TEM images of the synthesized large gold nanoparticles; (a + b) citrate coordinated gold nanoparticles with an average diameter of 14 nm; (c + d) TEM images of **GP-03** coordinated gold nanoparticles.

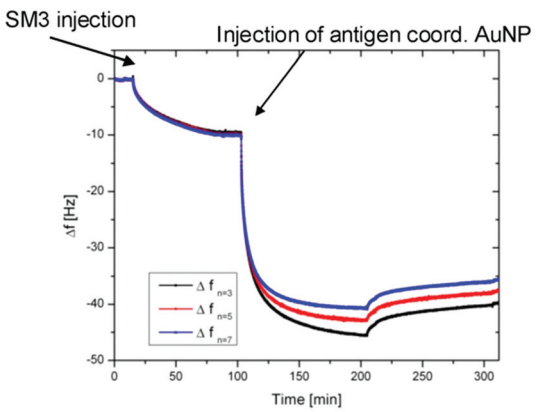

Fig. 7 Results of QCM measurements: QCM frequency shift *vs.* time for the binding of the **GP-02** coordinated AuNP to the preadsorbed SM3 antibody.

secondary antibody was added and incubated for 1 h at room temperature, before the substrate solution was finally added.

After adding the substrate solution, the horseradish peroxidase conjugated to the second antibody oxidized 3,3′,5,5′-tetramethylbenzidine (TMB) in the presence of H_2O_2 into a radical cation that forms a charged transfer complex with the unoxidized TMB. This blue complex led to dark stains in the spots containing the **GP-02** coordinated AuNP (Fig. 9b). These dark spots, visible to the naked eye, developed within minutes and indicated an antigen–antibody binding. The absence of color or change in color in the reaction of the negative control and the **GP-01** experiment revealed that this antigen–antibody binding is selective and specific for the binding of the glycosylated MUC1 partial structures with the full 20 amino acids containing the TR domain.

A qualitative detection of the antigen–antibody binding through a pale dot was still possible for the 1 : 50 dilution of

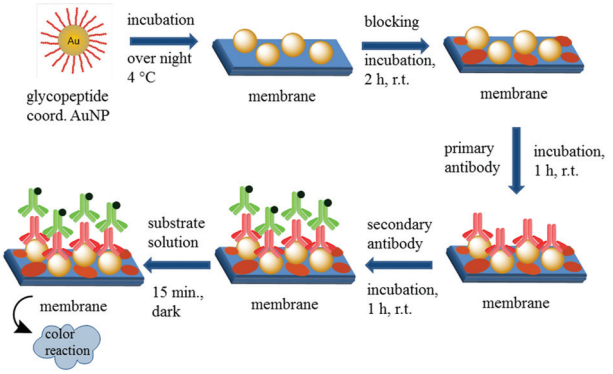

Fig. 8 Schematic process of the dot-blot immunoassay.

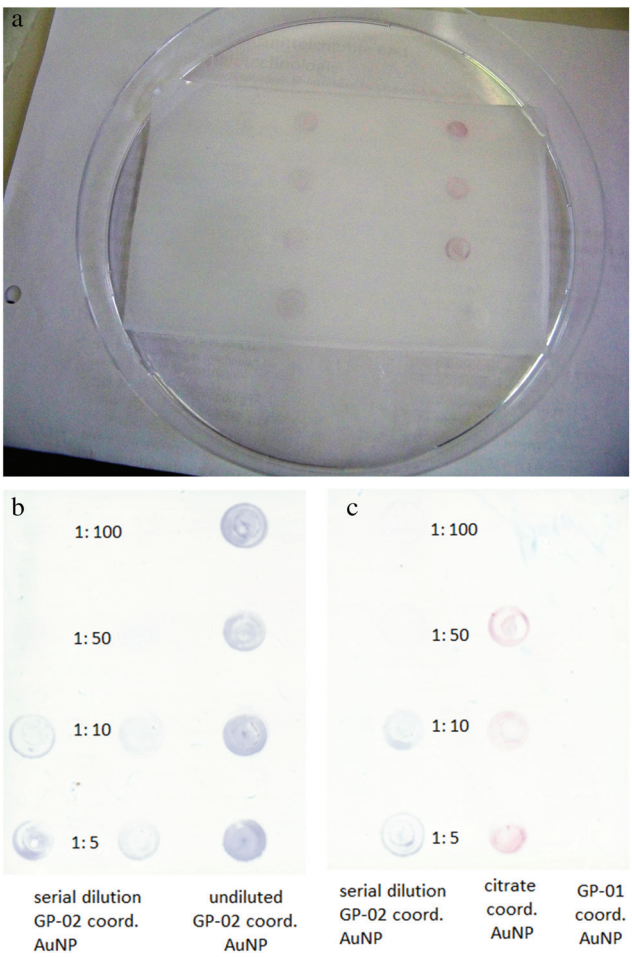

Fig. 9 Qualitative results of the dot-blot immunoassay (a) dot-blot immunoassay before the staining with the color reaction; (b) comparison of the binding affinities of **GP-02**, citrate and **GP-01** coord., AuNP after the staining reaction; (c) comparison of diluted and undiluted **GP-02** coord., AuNP after the staining reaction.

GP-02 coordinated AuNP (Fig. 9c). As the concentration of the serial dilution increases, the color of the blotted dots changes from pale to strong. Therefore, we can speculate that this method is sensitive even at low concentrations of the glycopeptide nanoparticle conjugates.

Conclusion

In this work we have successfully synthesized three different MUC1-glycopeptides using solid-phase peptide synthesis to assemble the individual components, such as the spacer or the T_N-antigen. These MUC1-glycopeptides were combined into potential vaccine candidates with gold colloids of different sizes in different synthetic ways, in order to override the natural tolerance of the immune system by multivalent presentation. The MUC1-glycopeptide immobilization on the gold colloid surface was characterized by TEM, UV/Vis spectra, DLS measurements, IR- and NMR-spectroscopy, which all indicated a high stability and solubility in water of the particles.

In addition, a novel dot-blot immunoassay was developed to analyze the nature of the antigen–antibody-binding of the MUC1-glycopeptide coord. gold colloids. Due to the strong affinity between the MUC1-glycopeptide and the SM3 antibody, blue dots can be visible to the naked eye without any instrument. The experimental results demonstrate that this new assay indicates a high selectivity, specificity and sensitivity for MUC1-glycopeptides containing the TR domain. These promising results suggest that gold colloids are robust and interesting platforms for presenting MUC1-glycopeptide antigens multivalently to their corresponding antibodies, which may lead to new potential developments in the construction of efficient immunotherapeutics, for example, antitumor vaccines.

Experimental section

Materials

All reactions of nanoparticles in aqueous solution were conducted in purified Millipore water. Organic solvents were distilled before use with the colloids. All other chemicals were purchased from commercial sources and used as received. The ligand exchange and coupling reactions were prepared under argon conditions. For peptide synthesis, all preloaded resins were obtained from Rapp Polymers GmbH (Tuebingen, Germany), the protected Fmoc-aminoacids were obtained from Orpengen Pharma (Heidelberg, Germany) and peptide grade solvents were purchased from Iris Biotech (Marktredwitz, Germany).

Instrumentation

The glycopeptides were synthesized on an automated ABI 433A peptide synthesizer (Applied Biosystems, Carlsbad, USA), which was equipped with an external 200 UV/Vis detector (Perkin Elmer) to control the synthesis process. Purification of the peptides was realized by the semi-preparative HPLC system (Jasco, Gross-Umstadt, Germany) consisting of two HPLC-pumps (type:PU-2087Plus), a degasser and a dynamic mixer.

Detection was applied with a Jasco UV/Vis-detector at 214 nm. A semi-preparative column purchased from Phenomenex (Torrance, USA) with the dimension 250 nm × 30 mm filled with Luna RP-C18(2), 100 A, Axia, 10 μm was used. All runs were performed at flow rates of 20.00 mL min^{-1}. As an eluent a mixture of acetonitrile and Millipore water both acidified with 0.1% TFA was used. Two different water–acetonitrile gradients were used: -gradient A: 95 : 5 at 0 min, 60 : 40 at 30 min, 0 : 100 at 40 min-gradient B: 75 : 25 at 0 min, 80 : 20 at 30 min, 0 : 100 at 40 min. All NMR spectra were recorded with a Bruker WT-300, a Bruker AM-400 and a Bruker Avance III 600 MHz spectrometer. Chemical shifts (δ) are given in ppm relative to TMS. Samples were prepared in deuterated solvents and their signals referenced to residual non-deuterated solvent signals. Because of the rigidity of the alkyl chains in the thiol shells and the resulting large differences in the relaxation times of different protons, no integrals are given for the proton NMR data of the gold colloids.

IR spectra were obtained on a Bruker IFS48 spectrometer in ATR mode. ESI-MS analyses were performed using a navigator instrument from Thermoelectronics with a sample concentration of 0.1 mg mL^{-1}, 0.75 mL min^{-1} flow rate, cone voltage 70 V, 45 V or 35 V and nitrogen flow rate 300 L min^{-1}. TEM measurements were performed on a Philips CM30 STEM (300 kV, LaB_6-cathode) equipped with a GATAN digital camera. TEM images were recorded using a digital micrograph. The average particle core sizes were determined by measuring at least 100 individual particles from recorded TEM images. The UV/Vis spectra were plotted with an Agilent 8453 spectrophotometer (Agilent Technologies Inc., Santa Clara, CA, USA). Dynamic light scattering measurements were performed with a StabiSizer PMX 200C from Particlemetrix (Meerbusch, Germany).

Quartz crystal microbalance (QCM). The QCM experiments were performed on a Qsense® D3000 microbalance. Quartz crystals with a resonance frequency of 5 MHz and with a 100 nm thick gold layer were used from Qsense. All experiments were performed at room temperature (T = 25 °C). The crystal was attached to the measurement chamber and immersed in PBS buffer. The respective antibody or antigen PBS solution was injected upon a constant frequency shift, followed by washing steps until the frequency shifts remained constant. All measurements were repeated three times.

Dot-blot immunoassay. Dot-blot immunoassay experiments were performed by a newly developed protocol. All measurements were performed in triplicate. 20 μL of the different AuNP samples were blotted onto the nitrocellulose membrane and incubated at 4 °C overnight. After three washing steps with a wash buffer (0.1% Tween 20 + PBS buffer pH 7.2) the rest sites of the nitrocellulose membrane were blocked with a block solution (1% milk powder in PBS buffer pH 7.2) by incubating for 2 h at room temperature. Then the membrane was washed three times with wash buffer, the primary anti-MUC1 antibody (monoclonal anti-MUC1, mouse lgG1 isotype from Sigma Aldrich) was added at a concentration of 2 μgmL^{-1} (20 μL antibody solution in 10 mL PBS buffer, pH 7.2) and the membrane was incubated for 1 h. After washing three times with wash buffer, the second antibody solution, which consists of a horseradish peroxidase conjugated goat–anti-mouse antibody from Biozym (Hessisch Oldendorf, Germany) diluted 10 000-fold in a wash buffer containing 0.5% BSA, was added and incubated for 1 h. For the substrate solution 1 mL of a TMB stock solution (1.2 mg 3,3′,5,5′-tetramethylbenzidine per mL of dimethyl sulfoxide) is filled up to 10 mL with sodium acetate buffer (18 mM, pH 4.5) and 0.05% (0.017 mL of a 30% solution) H_2O_2 was added. The membrane was covered with the substrate solution and incubated in the dark for 15 min.

Synthesis of 3,4,6-tri-*O*-acetyl-2-azido-2-deoxy-α-D-galactopyranosylbromide (αAc_3N_3GalBr) (1).[36] 29.10 g (335.0 mmol) lithium bromide was dissolved in 280 mL of acetonitrile and was put dropwise into a solution of 24.00 g (64.00 mmol) α/β$Ac_3N_3GalONO_2$ (ref. 31) in 120 mL of acetonitrile. The reaction mixture was stirred for 17 h at room temperature followed by dilution in 500 mL of dichloromethane before treatment with brine (2 × 250 mL) and drying with magnesium sulfate. Solvent removal left a yellow product, which was purified by flash chromatography with silica (cHex–EtOAc, 1 : 1); yield: 20.42 g (52.00 mmol, 81%); R_f = 0.58 (cHex–EtOAc, 1 : 1). $C_{12}H_{16}BrN_3O_7$ (M = 394.18 g mol^{-1}) [393.02].

^{1}H-NMR (300 MHz, $CDCl_3$): δ (ppm) = 6.47 (d, 1H, JH1,H2 = 3.9 Hz, 1-H), 5.50–4.48 (m, 1H, 4-H), 5.33 (dd, 1H, JH3,H4 = 3.6 Hz, JH3,H2 = 10.8 Hz, 3-H), 4.50–4.45 (m, 1H, 5-H), 4.20–4.06 (m, 2H, 6a,b-H), 3.98 (dd, 1H, JH2,H1 = 3.8 Hz, JH2, H3 = 10.7 Hz, 2-H), 2.15, 2.06, 2.05 (3 × s, 9H, 3 × CH_3 (Ac)).

***N*-[(9*H*-Fluoren-9-ylmethoxy)carbonyl]-L-threonine-*tert*-butyl ester; (Fmoc-Thr-O*t*Bu) (2).**[37] 45.00 g (218.0 mmol) *N*,*N*′-dicyclohexylcarbodiimide, 21.60 g (291.0 mmol) *tert*-butanol and 0.80 g (7.01 mmol) copper(I)-chloride were stirred for five days under an argon atmosphere and exclusion of light. Then 90 mL of dichloromethane was added and chilled to 0 °C while under Ar. 25.00 g (73.00 mmol) Fmoc-Thr-OH in 60 mL of dichloromethane was added dropwise through a septum over 40 min. The reaction mixture was cooled to room temperature with continued stirring. After 30 min the mixture was filtered through Hyflo® and 150 mL of cold dichloromethane was added. The filtrate was extracted thrice with 200 mL of a saturated sodium hydrogen carbonate solution, followed by washing twice with 200 mL of brine solution. The aqueous layer was separated from the organic layer, which was dried with magnesium sulfate and filtered. The solvent was removed *in vacuo* and purification was done by flash chromatography with silica (cHex–EtOAc, 4 : 1 → 2 : 1); yield: 16.38 g (41.00 mmol, 56%); R_f = 0.61 (cHex–EtOAc, 2 : 1). $C_{23}H_{27}NO_5$ (M = 397.46 g mol^{-1}) [397.19].

^{1}H-NMR (300 MHz, $CDCl_3$): δ (ppm) = 7.77 (d, 2H, JH4,H3 = JH5,H6 = 7.2 Hz, 4-H-, 5-H-Fmoc), 7.63–7.60 (m, 2H, 1-H-, 8-H-Fmoc), 7.40 (t, 2H, JH3,H2/H4 = JH6,H5/H7 = 7.4 Hz, 3-H-, 6-HFmoc),7.34–7.28 (m, 2H, 2-H-, 7-H-Fmoc), 5.59 (d, 1H, JNH, Tα = 8.7 Hz, NH), 4.41 (d, 2H, JCH,CH_2 = 7.2 Hz, CH_2 (Fmoc)), 4.33 (m, 1H, 9-H-Fmoc), 4.31–4.22 (m, 2H, Tα, Tβ), 2.08 (sb,1H, OH), 1.43 (s, 9H, CH_3 (*t*Bu)), 1.24 (d, 3H, JTγ,Tβ = 6.3 Hz, Tγ).

***N*-[(9*H*-Fluoren-9-ylmethoxy)carbonyl]-*O*-(3,4,6-tri-*O*-acetyl-2-azido-2-deoxy-α-D-galactopyranosyl)-L-threonine-*tert*-butyl ester (Fmoc-Thr-(αAc$_3$N$_3$Gal)-O*t*Bu) (3).**[38] A solution of 10.73 g (26.00 mmol) Fmoc-Thr-O*t*Bu **2** in 100 mL of dichloromethane–toluene (1 : 1) was stirred for 1 h with activated powdered molecular sieves (4 Å) under an argon atmosphere and exclusion of light. Then the mixture was cooled to 0 °C and 7.74 g (28.07 mmol) Ag_2CO_3 and 1.22 g (5.43 mmol) $AgClO_4$ in 8 mL of toluene were added. The mixture was stirred for 30 min at 0 °C before 10.00 g (0.025 mol) αAc$_3$N$_3$Gal-Br **1** in toluene (35 mL) and dichloromethane (35 mL) was added dropwise to the mixture over 90 min. After stirring overnight at room temperature, the mixture was diluted with 100 mL dichloromethane and filtered through Hyflo®. Then the filtrate was extracted twice with 150 mL of a saturated sodium hydrogen carbonate solution, followed by washing twice with 200 mL of brine solution. The aqueous layer was separated from the organic layer, which was dried with magnesium sulfate and filtered. The solvent was removed *in vacuo* and the crude product was purified by flash chromatography with silica (CH_2Cl_2–EtOAc, 10 : 1). Yield: 7.92 g (11.00 mmol, 45%), R_f = 0.74 (CH_2Cl_2–EtOAc, 10 : 1).

$C_{35}H_{42}N_4O_{12}$ (M = 710.73 g mol^{-1}) [710.28].

^{1}H-NMR (300 MHz, $CDCl_3$): δ (ppm) = 7.75 (d, 2H, *J*H4,H3 = *J*H5,H6 = 7.5 Hz, 4-H-, 5-H-Fmoc), 7.64 (d, 2H, *J*H1,H2 = *J*H7, H8 = 7.3 Hz, 1-H-, 8-H-Fmoc), 7.40 (t, 2H, *J*H3,H2/H4 = *J*H6, H5/H7 = 7.44 Hz, 3-H-, 6-H-Fmoc), 7.34–7.28 (m, 2H, 2-H-, 7-H-Fmoc), 5.66 (d, 1H, *J*NH,Tα = 9.3 Hz, NH (Fmoc)), 5.47 (d, 1H, *J*H4,H3 = 2.7 Hz, 4-H), 5.35 (dd, 1H, *J*H3,H4 = 3.0 Hz, *J*H3, H2 = 11.2 Hz, 3-H), 5.11 (d, 1H, *J*H1,H2 = 3.7 Hz, 1-H), 4.46–4.43 (m, 1H, Tβ), 4.40–4.36 (m, 2H, 6a,b-H), 4.32–4.25 (m, 3H, Tα, 5-H, 9-H-Fmoc), 4.10 (d, 1H, *J*CH$_2$,CH = 6.3 Hz, CH$_2$ (Fmoc)), 3.64 (dd,1H, *J*H2,H1 = 3.4 Hz, *J*H2,H3 = 11.0 Hz, 2-H), 2.15, 2.08, 2.04 (3 × s, 9H, 3 × CH_3 (Ac)), 1.51 (s, 9H, CH_3 (*t*Bu)), 1.36 (d, 3H, *J*Tγ,Tβ = 6.5 Hz, Tγ).

***N*-[(9*H*-Fluoren-9-ylmethoxy)carbonyl]-*O*-(2-acetamido-3,4,6-tri-*O*-acetyl-2-deoxy-α-D-galactopyranosyl)-L-threonine-*tert*-butyl ester (Fmoc-Thr-(αAc$_3$GalNAc)-O*t*Bu) (4).**[38] 4.51 g (69.00 mmol) zinc was activated with 2% aq. $CuSO_4$ solution and added to a mixture of 2.71 g (3.82 mmol) Fmoc-Thr-(αAc$_3$N$_3$Gal)-O*t*Bu **3** in 160 mL of THF–acetic anhydride–acetic acid (3 : 2 : 1). The mixture was then stirred at room temperature for 3 h. After completion of the reaction, the mixture was diluted with 500 mL, filtered through Hyflo®, concentrated and purified by flash chromatography with silica (cHex–EtOAc, 1 : 2). Yield: 1.63 g (2.24 mmol, 59%); R_f = 0.24 (cHex–EtOAc, 1 : 2). $C_{37}H_{46}N_2O_{13}$ (M = 726.77 g mol^{-1}) [726.30].

^{1}H-NMR (300 MHz, $CDCl_3$), δ (ppm) = 7.73 (d, 2H, *J*H4,H3 = *J*H5,H6 = 7.3 Hz, 4-H-, 5-H-Fmoc), 7.62 (d, 2H, *J*H1,H2 = *J*H7, H8 = 7.1 Hz, 1-H-, 8-H-Fmoc), 7.39 (t, 2H, *J*H3,H2/H4 = *J*H6, H5/H7 = 7.4 Hz, 3-H-, 6-H-Fmoc), 7.33–7.30 (m, 2H, 2-H-, 7-H-Fmoc), 5.99 (d, 1H, *J*NH,Tα = 9.9 Hz, NH (Fmoc)), 5.55 (d, 1H, *J*NH,H2 = 8.9 Hz, NH (GalNAc)), 5.38 (d, 1H, *J*H4,H3 = 2.4 Hz, 4-H), 5.07 (dd, 1H, *J*H3,H4 = 2.4 Hz, *J*H3,H2 = 10.7 Hz, 3-H), 4.86 (d, 1H, *J*H1,H2 = 2.7 Hz, 1-H), 4.62–4.57 (m, 1H, 2-H), 4.46–4.35 (m, 2H, CH_2 (Fmoc)), 4.27–4.04 (m, 6H, 9-H-Fmoc, 5-H, 6a,b-H, Tα, Tβ), 2.14 (s, 3H, CH_3 (Ac)), 2.02 (s, 3H, CH_3 (AcNH)), 1.98 (2 × s, 6H, 2 × CH_3 (Ac)), 1.44 (s,9H, CH_3 (*t*Bu)), 1.30 (d, 3H, *J*Tγ,Tβ = 6.0 Hz, Tγ).

***N*-[(9*H*-Fluoren-9-ylmethoxy)carbonyl]-*O*-(2-acetamido-3,4,6-tri-*O*-acetyl-2-deoxy-α-D-galactopyranosyl)-L-threonine (Fmoc-Thr-(αAc$_3$GalNAc)-OH) (5).**[38] 1.25 g (1.72 mmol) Fmoc-Thr-(αAc$_3$GalNAc)-O*t*Bu **4** was dissolved in 8 mL of dichloromethane and mixed with 15 mL of TFA and 2.5 mL of Millipore-H_2O. The mixture was stirred for 5 h at room temperature under an argon atmosphere. Then it was diluted in 30 mL of toluene. The crude product was concentrated to dryness, diluted in toluene, concentrated three times and purified by flash chromatography with silica (CH_2Cl_2–MeOH–AcOH, 95 : 5 : 1) to yield compound **5** (618 mg, 0.92 mmol, 54%); R_f = 0.10 (CH_2Cl_2–MeOH–AcOH, 95 : 5 : 1).

$C_{33}H_{38}N_2O_{13}$ (M = 670.66 g mol^{-1}) [670.24].

^{1}H-NMR (300 MHz, $CDCl_3$), δ (ppm) = 7.76 (d, 2H, *J*H4,H3 = *J*H5,H6 = 7.2 Hz, 4-H-, 5-H-Fmoc), 7.62 (d, 2H, *J*H1,H2 = *J*H7, H8 = 7.3 Hz, 1-H-, 8-H-Fmoc), 7.39 (t, 2H, *J*H3,H2/H4 = *J*H6, H5/H7 = 7.2 Hz, 3-H-, 6-H-Fmoc), 7.33–7.30 (m, 2H, 2-H-, 7-H-Fmoc), 6.05 (d, 1H, *J*NH,Tα = 8.9 Hz, NH(Fmoc)), 5.91 (d, 1H, *J*NH,H2 = 9.3 Hz, NH (GalNAc)), 5.38 (d, 1H, *J*H4,H3 = 2.9 Hz, 4-H), 5.14 (dd, 1H, *J*H3,H4 = 2.7 Hz, *J*H3,H2 = 11.2 Hz, 3-H), 4.98 (d, 1H, *J*H1,H2 = 3.3 Hz, 1-H), 4.66–4.58 (m, 1H, 2-H), 4.52–4.38 (m, 2H, CH_2 (Fmoc)), 4.29–4.04 (m, 6H, 9-H-Fmoc, 5-H, 6a,b-H, Tα,Tβ), 2.17 (s, 3H, CH_3 (Ac)), 2.04 (s, 3H, CH_3 (AcNH)), 1.98 (2× s, 6H, 2× CH_3 (Ac)), 1.29 (d, 3H, *J*Tγ,Tβ = 6.2 Hz, Tγ).

12-Hydroxy-4,7,10-trioxadodecanoic acid *tert*-butyl ester (HO(CH$_2$CH$_2$O)$_3$CH$_2$CH$_2$COO*t*Bu) (6).[39] To a solution of 25.6 mL (188.0 mmol) anhydrous triethyleneglycol in 100 mL of THF were added 40 mg (0.90 mmol) of sodium. When the sodium was dissolved, 9.6 mL of (66.00 mmol) *tert*-butyl acrylate was added and then the mixture was stirred for 20 h and then neutralized with 8 mL of 1 M HCl. After removal of the solvent, the residue was suspended in 100 mL of brine solution and extracted thrice with 50 mL of ethyl acetate. The combined organic layers were dried over magnesium sulfate before the solvent was removed. The resulting colorless oil was dried *in vacuo* to give a yield of 15.75 g (57.00 mmol, 86%); R_f = 0.32 (EtOAc). $C_{13}H_{26}O_6$ (M = 278.34 g mol^{-1}) [278.17].

^{1}H-NMR (300 MHz, $CDCl_3$), δ (ppm) = 3.72–3.69 (m, 4H, 3-CH_2, 14-CH_2), 3.67–3.58 (m, 10H, 5 × OCH_2), 2.50 (t, 2H, *J*CH$_2$, CH$_2$ = 6.7 Hz, 2-CH_2), 1.43 (s, 9H, *t*Bu).

12-Azido-4,7,10-trioxadodecanoic acid *tert*-butyl ester (N$_3$(CH$_2$CH$_2$O)$_3$CH$_2$CH$_2$COO*t*Bu) (7).[39] 15.60 g (0.056 mol) of compound **6** was dissolved in 20 mL of dichloromethane and 19.2 mL of (136.2 mmol) NEt_3 was added. Under cooling in an ice-bath, 8.9 mL of (116.1 mmol) MsCl was added dropwise. After stirring for 4 h, precipitated NEt_3·HCl was filtered through Hyflo® and the filtrate was extracted twice with 25 mL of dichloromethane, washed thrice with 25 mL of ice-water and twice with brine solution. Then the organic layers were dried with magnesium sulfate and filtered. The solvent was removed *in vacuo* and the remaining residue was dissolved in 20 mL of DMF and mixed with 22.46 g (345.52 mmol) NaN_3.

After the stirring was continued for 17 h at 60 °C, the solvent was evaporated *in vacuo* and the remaining residue was dissolved in 50 mL of H_2O. The solution was extracted five times with 40 mL of Et_2O. The solvent was removed *in vacuo* and the crude product was purified by flash chromatography with silica (cHex–EtOAc, 3 : 1) to yield 9.63 g (31.00 mmol, 57%) of a yellow oil. R_f = 0.22 (cHex–EtOAc, 3 : 1).

$C_{13}H_{25}N_3O_5$ (M = 303.35 g mol^{-1}) [303.18].

^{1}H-NMR (300 MHz, $CDCl_3$): δ (ppm) = 3.73–3.68 (m, 4H, 3-CH_2, 14-CH_2), 3.67–3.58 (m, 10H, 5 × OCH_2), 2.49 (t, 2H, $J$$CH_2$,$CH_2$ = 6.9 Hz, 2-CH_2), 1.44 (s, 9H, *t*Bu).

12-Amino-4,7,10-trioxadodecanoic acid *tert*-butyl ester (H_2N-$(CH_2CH_2O)_3CH_2CH_2COOtBu$) (8).[39] To a suspension of 7.17 g RANEY® nickel alloy in 250 mL of H_2O, solid NaOH was added until the foaming stopped. After 10 min at room temperature the mixture was heated to 70 °C for 30 min. Subsequently, the mixture was decanted from the RANEY® nickel, which then was washed with H_2O until pH 8 was reached. The catalyst was washed thrice with 150 mL of i-PrOH, before 9.55 g (315 mmol) ($N_3(CH_2CH_2O)_3CH_2CH_2COOtBu$) **7** dissolved in 150 mL of i-PrOH was added. The mixture was degassed *in vacuo*, flooded with Ar and then stirred under a H_2 atmosphere for 15 h. The catalyst was filtered off through Hyflo® and the filtrate was washed with 30 mL of i-PrOH. The solvent was removed *in vacuo* and 8.33 g (30.00 mmol, 95%) of a yellow oil was yielded. R_f = 0.16 (cHex–EtOAc, 2 : 1).

$C_{13}H_{27}NO_5$ (M = 277.36 g mol^{-1}) [277.19].

***N*-[(9*H*-Fluoren-9-ylmethoxy)carbonyl]-amido-4,7,10-trioxadodecanoic acid *tert*-butyl ester (Fmoc-NH$(CH_2CH_2O)_3$-$CH_2CH_2COOtBu$) (9).**[40] 8.33 g (0.030 mol) of compound **8** was dissolved in 250 mL of acetone–H_2O (1 : 1) and then 2.53 g (30.80 mmol) sodium hydrogen carbonate was added. After adding 10.30 g (30.60 mmol) Fmoc-Os slowly to the reaction mixture, it was then vigorously stirred at room temperature for 90 h. HCl was added until pH 6 was reached, before acetone was evaporated. After phase separation, the aqueous layer was extracted four times with 100 mL of dichloromethane. The combined organic layers were washed with 250 mL of 1 M HCl, 250 mL of H_2O and dried with magnesium sulfate. The solvent was removed *in vacuo* and the crude product was purified by flash chromatography with silica (cHex–EtOAc, 2 : 1 → 1 : 1 → 1 : 2). Yield: 7.62 g (15.20 mmol, 51%); R_f = 0.22 (cHex–EtOAc, 2 : 1).

$C_{28}H_{37}NO_7$ (M = 499.60 g mol^{-1}) [499.26].

^{1}H-NMR (300 MHz, CDCl3): δ (ppm) = 7.76 (d, 2H, JH4,H3 = JH5,H6 = 7.9 Hz, 4-H-, 5-H-Fmoc), 7.60 (d, 2H, JH1,H2 = JH8, H7 = 7.4 Hz, 1-H-, 8-H-Fmoc), 7.42–7.14 (m, 4H, 2-H-, 3-H-, 6-H-, 7-H-Fmoc), 4.38 (d, 2H, $J$$CH_2$,CH = 6.9 Hz, CH_2-Fmoc), 4.20 (t, 1H, 9-H-Fmoc, JH9,CH_2 = 6.8 Hz),3.76–3.49 (m, 12H, 6 × OCH_2), 3.41 (t, 2H, $J$$CH_2$,$CH_2$ = 5.4 Hz, 12-CH_2), 2.60 (t, 2H, $J$$CH_2$,$CH_2$ = 6.7 Hz, 2-CH_2), 1.43 (s, 9H, CH_3-*t*Bu).

***N*-[(9*H*-Fluoren-9-ylmethoxy)carbonyl]amido-4,7,10-trioxadodecanoic acid (Fmoc-NH$(CH_2CH_2O)_3CH_2CH_2COOH$) (10).**[40] 7.5 g (15.00 mmol) (Fmoc-NH$(CH_2CH_2O)_3CH_2CH_2COOtBu$) **9** in 56 mL of TFA and 5.5 mL of H_2O was stirred at room temperature for 3 h. After dilution with 50 mL of toluene, the solvents were evaporated *in vacuo* and thrice 30 mL of toluene and twice 30 mL of dichloromethane were co-distilled from the remainder. The crude product was purified by flash chromatography with silica (CH_2Cl_2–MeOH–EtOAc, 19 : 1 : 0.5). Yield: 4.61 g (10.40 mmol, 69%); R_f = 0.32 (CH_2Cl_2–MeOH–EtOAc, 19 : 1 : 0.5). $C_{24}H_{29}NO_7$ (M = 443.49 g mol^{-1}) [443.19].

^{1}H-NMR (300 MHz, $CDCl_3$): δ (ppm) = 7.77 (d, 2H, JH4,H3 = JH5,H6 = 7.9 Hz, 4-H-, 5-H-Fmoc), 7.60 (d, 2H, JH1,H2 = JH8, H7 = 7.4 Hz, H-1-, H-8-Fmoc), 7.42–7.14 (m, 4H, 2-H-, 3-H-, 6-H-, 7-H-Fmoc), 6.40 (sb, 1H, NH-Fmoc), 4.39 (d, 2H, $J$$CH_2$,CH = 6.7 Hz, CH_2-Fmoc), 4.20 (t, 1H, 9-H-Fmoc, JH9,CH_2 = 6.7 Hz), 3.71 (t, 2H, $J$$CH_2$,$CH_2$ = 5.8 Hz, 11-CH_2), 3.68–3.49 (m, 10H, 5 × OCH_2), 3.47–3.36 (m, 2H, 12-CH_2), 2.60 (t, 2H, $J$$CH_2$,$CH_2$ = 6.7 Hz, 2-CH_2).

Standard protocol of the glycopeptide synthesis

The glycopeptides were synthesized using a standard fluorenyl-methoxycarbonyl (Fmoc) chemistry protocol with 454.5 mg Fmoc-Pro-*O*-Trt Tentagel resin (Rapp Polymere, 0.22 mmol g^{-1}). The standard coupling of an amino acid was performed in a three-part cycle of coupling. In the first step the Fmoc protecting group of the starting amino acid was cleaved with 20% solution of piperidine in NMP and then in the next step, 1.00 mmol (10 eq.) of the Fmoc-amino acid was activated with a solution of 1.00 mmol HBTU, 1.00 mmol HOBt and 2.00 mmol DIPEA in NMP. The coupling time was 20 min at room temperature. The third step, the capping, was carried out by acetic anhydride, while all free amino groups were acetylated. After the capping step, the cycle began with the removal of the terminal Fmoc protecting group again. After the last amino acid the Fmoc group was removed again and the resin was thoroughly washed with NMP and dichloromethane. Finally the glycopeptides were cleaved from the resin with 10 mL of trifluoroacetic acid, 1 mL of triisopropylsilane and 1 mL of water and the solution was washed three times with 3 mL of trifluoroacetic acid.

The entire filtrate was treated with 20 mL of toluene and concentrated *in vacuo* by evaporating the solvent. The residue was co-distilled five-times with toluene and then dissolved in 10 mL of water and lyophilized.

Amino-4,7,10-trioxadodecanylamido-*N*-L-prolyl-L-alanyl-L-histidyl-L-glycyl-L-valyl-*O*-(2-acetamido-3,4,6,-tri-*O*-acetyl-2-desoxy-α-D-galactopyranosyl)-L-threonyl-L-seryl-L-alanyl-L-proline (H_2N-$(CH_2CH_2O)_3CH_2CH_2CONH$-Pro-Ala-His-Gly-Val-Thr(αAc_3GalNAc)-Ser-Ala-Pro-OH) (11). To synthesize the glycopeptide **11** the peptide was assembled using the above described standard protocol. The coupling of the saccharide-amino acid building block compound **5** was carried out manually in the synthesizer's vessel. For this purpose, the terminal Fmoc group was removed through treatment with a 20% solution of piperidine in NMP. Subsequently, a solution of 134.1 mg (0.2 mmol, 2.0 eq.) **5**, 91.2 mg (0.24 mmol, 2.4 eq.) HATU, 32.7 mg (0.24 mmol, 2.4 eq.) HOAt and 55 μL (0.5 mmol, 5 eq.) NMM in NMP (2 mL) was added to the resin and strongly shaken for 8 h (30 s Vortex, 30 s stop), followed by filtration and washing with NMP and dichloromethane. The remaining free amino

groups were acetylated with capping reagents. The coupling of the next amino acid was performed twice following the standard protocol. All further amino acids were coupled according to the standard protocol. The spacer-amino acid coupling was carried out manually as described above using 88.7 mg (0.2 mmol, 2.0 eq.) 10 HATU (2.4 eq.), HOAt (2.4 eq.) and NMM (5 eq.) in NMP (2 mL) and strongly shaken for 4 h. The N-terminal Fmoc group of the spacer-amino acid was removed on resin by applying a solution of 20% piperidine in NMP three times for 2.5 min followed by washing with NMP and dichloromethane. The resin was transferred to a Merrifield-solid phase-vessel and 10 mL of a solution of trifluoroacetic acid–triisopropylsilane–water (10 : 1 : 1) was added. The vessel was shaken for 3 h. The solution was filtered, and the resin was washed two times with 2 mL trifluoroacetic acid. Toluene (20 mL) was added to the combined solutions, the solvent was removed *in vacuo*, and the residue was co-distilled two times with toluene (20 mL) and lyophilized. The lyophilisate was directly used in the next step, without further purification.

Yield: 59 mg (0.043 mmol, 43%), colorless lyophilisate. R_t = 16.14 min (Phenomenex Luna, gradient see Instrumentation) $C_{59}H_{93}N_{13}O_{24}$ (M = 1368.44 g mol^{-1}) [1367.65].

ESI-MS (positive), m/z: 1368.66 ([M + H]$^+$, ber.: 1368.65), 684.84 ([M + 2H]$^{2+}$, ber.: 684.83).

Amino-4,7,10-trioxadodecanyl-amido-*N*-L-prolyl-L-alanyl-L-histidyl-L-glycyl-L-valyl-*O*(-2acetamido-2-deoxy-α-D-galactopyranosyl)-L-threonyl-L-seryl-L-alanyl-L-proline ($H_2N(CH_2CH_2O)_3CH_2CH_2$-CONH-Pro-Ala-His-Gly-Val-Thr(αGalNAc)-Ser-Ala-Pro-OH) (GP-01). To remove the carbohydrate protecting groups the glycopeptide **11** was dissolved in 25 mL of methanol and a solution of 0.5 g sodium in 25 mL of methanol was added dropwise until the pH reached 10.5. After stirring for 18 h at room temperature the mixture was neutralized with three drops of concentrated acetic acid, before the solvent was evaporated *in vacuo*. The crude product was purified by a semi-preparative RP-HPLC.

Yield: 44 mg (0.035 mmol, 82%) colorless lyophilisate; R_t = 10.34 min (Phenomenex Luna, gradient A see Instrumentation).

$C_{53}H_{87}N_{13}O_{21}$ (M = 1242.33 g mol^{-1}) [1241.61].

ESI-MS (positive), m/z: 1242.61 ([M + H]$^+$, ber.: 1242,62), 621.79 ([M + 2H]$^{2+}$, ber.: 621.81).

^{1}H-NMR (400 MHz, D_2O, COSY, HSQC): δ (ppm) = 8.52 (d, 1H, JHε,Hδ = 1.25 Hz, Hε), 7.22 (, 1H, JHδ,Hε = 1.43 Hz, Hδ), 4.83 (d, 1H, JH1,H2 = 3.91 Hz, H1), 4.85–4.11 (m, 9H, Hα{4.60}, Tα{4.52}, A1α {4.39}, Sα{4.38}, P1α{4.31}, P2α{4.26}, Tβ{4.21}, Vα{4.20}, A2α{4.12}), 3.98 (dd, 1H, JH2, H1 = 3.95 Hz, JH2,H3 = 10.58 Hz, H2), 3.93–3.33 (m, 27H, H5 {3.89}, Gαa {3.85}, Gαb{3.84}, H4 {3.83}, H3 {3.74}, H6a,b{3.68}, 3-CH_2-Spacer {3.67}, Sβ{3.65}, 5 × CH_2O-Spacer {3.62}, P1δ{3.55}, P2δ{3.53}, 2-CH_2-Spacer {3.45}), 3.20 (dd, 1H, JHβ,Hα = 5.64 Hz, Hβ), 3.08 (m, 2H, CH_2-Spacer), 2.70–2.52 (m, 4H, 12-CH_2-Spacer {2.65}, 2-CH_2-Spacer {2.57}), 2.31–2.07 (m, 4H, P1β{2.22}, P2β{2.15}), 2.05–1.70 (m, 5H, Vβ{1.99}, P1γ{1.91}, P2γ{1.89}), 1.32–1.19 (m, 6H, A1β{1.28}, A2β{1.23}), 1.16 (d, 3H, JTγ,Hβ = 6.41 Hz, Tγ), 0.86 (t, 6 H, JVγ,Vβ = 6.34 Hz, Vγ).

^{13}C-NMR (100.6 MHz, D_2O, HSQC): δ (ppm) = 175.9, 174.9, 174.4, 173.7, 172.9, 172.4, 172.0, 171.5, 171.1, 170.9, 170.6 (C═O, C═O–acetyl), 163.1 (C═NH), 133.4 (Hε), 128.4 (Hγ), 117.2 (Hδ), 99.0 (C1), 76.8 (Tβ), 71.3 (C5), 69.6, 69.5, 69.5, 69.4 (CH_2O-Spacer), 68.5 (C4), 68.2 (C3), 66.3 (S), 61.3 (11-CH_2-Spacer), 60.0 (P2α), 59.5 (P1α), 59.4 (Vα), 57.0 (Tα), 54.9 (Sα), 52.3 (Hα), 49.6 (C2), 49.6 (A2α), 48.7, 48.0 (2-CH_2-Spacer), 47.7 (P2δ), 47.6 (A1α), 47.5 (P1δ), 47.4 (C6), 42.3 (Gα), 39.0, 34.0 (12-CH_2-Spacer), 30.1 (Vβ), 29.6 (P2β), 28.7 (P1β), 28.7 (P2γ), 28.6 (P1γ), 26.2 (Hβ), 22.2 (CH_3-AcNH), 18.4 (Tγ), 18.24 (Vγb), 17.7 (Vγa), 16.3 (A2β), 15.0 (A1β).

Amino-4,7,10-trioxadodecanylamido-*N*-L-prolyl-L-alanyl-L-histidyl-L-glycyl-L-valyl-*O*-(2-acetamido-2-desoxy-α-D-galactopyranosyl)-L-threonyl-L-seryl-L-alanyl-L-prolyl-L-aspartyl-L-threonyl-L-arginyl-L-prolyl-L-alanyl-L-prolyl-L-glycyl-L-seryl-L-threonyl-L-alanyl-L-proline ($H_2N(CH_2CH_2O)_3CH_2CH_2CONH$-Pro-Ala-His-Gly-Val-Thr(αGNAc)-Ser-Ala-Pro-Asp-Thr-Arg-Pro-Ala-Pro-Gly-Ser-Thr-Ala-Pro-OH) (GP-02). To synthesize the glycopeptide **GP-02** the peptide was assembled using the above described standard protocol. The coupling of the saccharide-amino acid building block compound **5** was carried out manually in the synthesizer's vessel. For this purpose, the terminal Fmoc group was removed through treatment with a 20% solution of piperidine in NMP. Subsequently, a solution of 134.1 mg (0.2 mmol, 2.0 eq.) **5**, 91.2 mg (0.24 mmol, 2.4 eq.) HATU, 32.7 mg (0.24 mmol, 2.4 eq.) HOAt and 55 μL (0.5 mmol, 5 eq.) NMM in NMP (2 mL) was added to the resin and strongly shaken for 8 h (30 s Vortex, 30 s stop), followed by filtration and washing with NMP and dichloromethane. The remaining free amino groups were acetylated with capping reagents. The coupling of the next amino acid was performed twice following the standard protocol. All further amino acids were coupled according to the standard protocol. The spacer–amino acid coupling was carried out manually as described above using 88.7 mg (0.2 mmol, 2.0 eq.) 10 HATU (2.4 eq.), HOAt (2.4 eq.) and NMM (5 eq.) in NMP (2 mL) and strongly shaken for 4 h. The N-terminal Fmoc group of the spacer–amino acid was removed on resin by applying a solution of 20% piperidine in NMP three times for 2.5 min followed by washing with NMP and dichloromethane. The resin was transferred to a Merrifield-solid phase-vessel and 10 mL of a solution of trifluoroacetic acid–triisopropylsilane–water (10 : 1 : 1) was added. The vessel was shaken for 3 h. The solution was filtered, and the resin was washed two times with 2 mL trifluoroacetic acid. Toluene (20 mL) was added to the combined solutions, the solvent was removed *in vacuo*, and the residue was co-distilled two times with toluene (20 mL) and lyophilized. The lyophilisate was directly used in the next step without further purification.

Yield: 128 mg (0.053 mmol, 53%), colorless lyophilisate. R_t = 13.64 min (Phenomenex Luna, gradient see Instrumentation). $C_{103}H_{163}N_{27}O_{40}$ (M = 2419.55 g mol^{-1}) [2418.16].

ESI-MS (positive), m/z: 1210.56 ([M + 2H]$^{2+}$, ber.: 1210.09).

To remove the carbohydrate protecting groups the glycopeptide was dissolved in 25 mL methanol and a solution of 0.5 g sodium in 25 mL methanol was added dropwise until the pH reached 10.5. After stirring for 18 h at room temperature

the mixture was neutralized with three drops of concentrated acetic acid, before the solvent was evaporated *in vacuo*. The crude product was purified by a semi-preparative RP-HPLC.

Yield: 45 mg (0.020 mmol, 20%) colorless lyophilisate. R_t = 8.67 min (Phenomenex Luna, gradient A see Instrumentation).

$C_{97}H_{157}N_{27}O_{37}$ (M = 2293.44 g mol^{-1}) [2292.12].

ESI-MS (positive), *m*/*z*: 1147.65 ([M + 2H]$^{2+}$ cal.: 1147.07), 765.11 ([M + 3H]$^{3+}$, cal.: 765.05), 1529.92 ([2M + 3H]$^{3+}$, cal.: 1529.10), 2294.35 ([M + H]$^{+}$, cal.: 2293.13).

HR-MS (positive), *m*/*z*: 1147.0693 ([M + 2H]$^{2+}$, cal.: 1147.0695).

^{1}H-NMR (400 MHz, MeOH-d$_4$, COSY, HSQC): δ (ppm) = 8.79 (d, 1H, *J*Hε,Hδ = 1.49 Hz, Hε), 7.43 (d, 1H, *J*Hδ, Hε = 1.43 Hz, Hδ), 5.02 (d, 1H, *J*H1,H2 = 3.63 Hz, H1), 4.70–4.21 (m, 21H, Dα {4.68}, Hα {4.66}, Rα {4.64}, A3α {4.63}, A2α {4.62}, S2α {4.59}, A4α {4.57}, S1α {4.54}, P1-5α {4.51, 4.50, 4.46, 4.45, 4.41}, Vα {4.39}, TTnα {4.36}, TTnβ {4.35}, A1α {4.32}, T1α {4.29}, T2α {4.27}, T2β {4.26}, T1β {4.24}), 4.17 (dd, 1H, *J*H2,H1 = 3.57 Hz, *J*H2,H3 = 10.80 Hz, H2), 4.10–3.60 (m, 31H, G1αa {4.08}, G1αb {4.05}, H5 {4.04}, S2β {4.01}, P1δ {3.95}, G2α {3.93}, S1β {3.85}, H3 {3.81}, H6a,b {3.78}, P1δ {3.76}, P2δ {3.75}, H4 {3.69}, 3-CH$_2$-Spacer {3.67}, 2-CH$_2$-Spacer {3.67}, 5 × CH$_2$O-Spacer {3.66}, P2-5δ {3.64, 3.63, 3.62}), 3.40 (d, 1H, *J*Hβ,Hα = 5.65 Hz, Hβa), 3.24–3.12 (m, 5H, CH$_2$-Spacer {3.22}, Hβb {3.20}, Dβa {3.17}, Rδ {3.12}), 2.92 (m, 1H, Dβb), 2.73–2.65 (m, 2H, 12-CH$_2$-Spacer), 2.31–2.20 (m, 4H, P1,2βa {2.27, 2.25}, CH$_2$-Spacer {2.24}), 2.18–2.09 (m, 4H, CH$_2$-Spacer), 2.08–1.84 (m, 21H, P3-5βa {2.07, 2.05, 2.04}, Vβ {2.03}, P1-5γ {2.02, 2.01}, P1-5βb {2.00}, Rβa {2.15}, AcNH {s, 1.86}), 1.74–1.64 (m, 3H, Rβb {1.70}, Rγ {1.68}), 1.43–1.29 (m, 12H, A2β {1.40}, A4β {1.37}, A3β {1.36}, A1β {1.35}), 1.26 (d, 3H, *J*Tγ,Tβ = 6.35 Hz, TTnγ), 1.22–1.14 (m, 6H, *J*Tγ,Tβ = 6.57 Hz, T1γ {1.20}, T2γ {1.18}), 0.99 (t, 6H, *J*Vγ,Vβ = 5.18 Hz, Vγ).

^{13}C-NMR (100.6 MHz, MeOH-d$_4$, HSQC): δ (ppm) = 173.8, 173.7, 173.7, 173.0, 173.0, 172.8, 172.6, 172.6, 172.3, 172.2, 173.1, 171.6, 171.5, 171.4, 171.2, 171.0, 170.9, 170.8, 170.55, 170.5, 170.4, 170.3 (C═O, C═O–acetyl), 157.0 (C═NH), 133.5 (Hε), 129.2 (Hγ), 117.4 (Hδ), 99.0 (C1), 76.4 (TTnβ), 70.0 (CH$_2$-Spacer), 69.9 (C3), 69.7 (C4), 68.9 (T1β), 66.8 (C5), 66.4 (T2β), 66.2 (C6), 61.7 (S1β), 61.5 (S2β), 61.3, 61.1, 60.3, 60.2, 60.1 (P1-5α), 59.8 (T2α), 58.9 (T1α), 58.7 (Vα), 58.4 (TTnα), 56.4 (S2α), 55.6 (S1α), 55.1 (Hα), 52.2 (Rα), 50.6 (Dα), 49.6 (C2), 48.3 (A3α), 48.1 (A1α), 47.9 (A4α), 47.7, 47.5, 47.2, 47.0, 46.9, 46.7 (P1-5δ), 42.3 (G2α), 41.9 (G1α), 40.6 (CH$_2$-Spacer), 39.1 (Rδ), 34.3 (Dβ), 30.1 (Vβ), 29.3, 29.1, 29.0, 28.8, 28.6 (P1-5β), 27.8 (Rβ), 26.4 (Hβ), 24.8, 24.6, 24.5, 24.4, 24.3 (P1-5γ), 24.1 (Rγ), 21.8 (CH$_3$-AcNH), 18.8 (T1γ), 18.7 (T2γ), 18.4 (Vγa), 17.8 (TTnγ), 17.5 (Vγb), 15.7, 15.5, 15.3, 15.0 (A1-4β).

Synthesis of the gold nanoparticles

Dodecanethiol coordinated gold nanoparticles with a diameter of 7 nm (AuDT) (12). 0.120 g (0.24 mmol) Au(PPh$_3$)Cl and 0.125 mL (0.50 mmol) of dodecanethiol were dissolved in 20 mL of benzene. 0.213 g (2.41 mmol) of *tert*-butylamine-borane complex was added to the solution and the mixture was stirred at 55 °C for 1 h, before it was cooled to room temperature. Then 20 mL of ethanol were added and the precipitant separated by centrifugation. The black solid powder was washed with ethanol at least three times, dried *in vacuo* and resolved in 20 mL chloroform. A dark red colloid solution with a particle concentration of 1.33 μM was obtained and stored at 4 °C.

DLS: d_h = 7 ± 1 nm; TEM: d = 7 ± 1 nm; UV/Vis: λ_{max} = 524 nm; ^{1}H-NMR (400 MHz, CDCl$_3$): δ = 0.88 (t, ^3J = 7,2 Hz, 3H, CH$_3$); 1.26–1.38 (bs, 20H, CH$_2$); 1.59 (bs, 2H, CH$_2$) ppm.

ATR-IR: 2916.1 cm^{-1} (s, νC–H)); 2849.0 cm^{-1} (s, νC–H)); 1455.7 cm^{-1} (m, δ(C–H)); 1433.8 cm^{-1} (m, δ(C–H)); 1404.8 cm^{-1} (m, δ(C–H)); 1378.4 cm^{-1} (m, δ(CH$_3$)); 720.5 cm^{-1} (w, CH$_2$-rocking).

***N*-Hydroxysuccinimide-11-mercaptoundecanoate (MUDHSE) (13).** 0.501 g (4.4 mmol) *N*-hydroxysuccinimide (NHS) was dissolved in 250 mL of dichloromethane. 0.952 g (4.4 mmol) 11-mercaptoundecanoic acid in 5 mL of dichloromethane and 0.988 g (4.8 mmol) *N*,*N*′-dicyclohexylcarbodiimide in 25 mL of dichloromethane were added dropwise and the mixture was stirred for 24 h at room temperature. The colorless solid precipitate was filtered off and the solvent was removed *in vacuo*. The residue was suspended in small amounts of DMF and the insoluble amount of residue was filtered off. The DMF was evaporated. Yield: 1.24 g (3.94 mmol, 89%).

^{1}H-NMR (400 MHz, DMSO-d$_6$): δ = 1.26–1.35 (m, CH$_2$); 1.49–1.64 (m, CH$_2$); 2.23 (m, SH); 2.46 (t, CH$_2$); 2.66 (t, CH$_2$); 2.81 (s, CH$_2$) ppm.; ^{13}C-NMR (100 MHz, DMSO-d$_6$): δ = 23.72 (CH$_2$); 24.25 (CH$_2$); 25.41 (CH$_2$); 27.71 (CH$_2$); 27.95 (CH$_2$); 28.43 (CH$_2$); 28.73 (CH$_2$); 28.81 (CH$_2$); 30.15 (CH$_2$); 30.74 (CH$_2$); 33.36 (CH$_2$); 35.75 (CH$_2$); 162.27 (CO); 168.97 (CO); 170.23 (CO) ppm.; ATR-IR: 2917.0 cm^{-1} (s,ν(C–H)); 2849.1 cm^{-1}(s,ν(C–H)); 1812.0 cm^{-1} (m,ν(C═O)); 1783.8 cm^{-1} (m,ν(C═O)); 1727.5 cm^{-1} (m,ν(C═O)); 1651.1 cm^{-1} (s,ν(C═O)); 1525.4 cm^{-1} (w, ν(O═C–N)); 1371.6 cm^{-1} (w, δ(C–H)); 1309.6 cm^{-1} (w, δ(C–H)); 1201.4 cm^{-1} (s,ν(C–O)); 1070.2 cm^{-1} (s, ν(C–O)).

***N*-Hydroxysuccinimide-11-mercaptoundecanoate coordinated gold nanoparticles with a diameter of 7 nm (MUDHSE coord. AuNP) (14).** MUDHSE coordinated gold nanoparticles were obtained by a ligand exchange reaction of the dodecanethiol coordinated gold nanoparticles with the new ligand. 0.190 g (0.31 mmol) *N*-hydroxysuccinimide-11-mercapto-undecanoate was dissolved in 40 mL of anhydrous DMF and next 6 mL (6 nmol) of dodecanethiol-protected gold nanoparticles dissolved in chloroform were added dropwise to the stirring solution. After 30 min 10 mL of the solution was removed under reduced pressure and the solution was stirred at room temperature for another 18 h. The particle solution was dialyzed against 600 mL DMF several times, dried *in vacuo* and resolved in 30 mL of anhydrous DMF and stored at 4 °C. A clear red solution with a particle concentration of 0.20 μM was obtained. DLS: d_h = 11 ± 2 nm; TEM: d = 7 ± 1 nm; UV/Vis: λ_{max} = 524 nm; ^{1}H-NMR (400 MHz, DMSO-d$_6$): δ = 1.25–1.41 (m, CH$_2$); 1.52 (quin, CH$_2$); 1.61 (quin, CH$_2$); 2.22 (m, CH$_2$); 2.65 (t, CH$_2$); 2.79 (s, CH$_2$) ppm; ATR-IR: 2922.4 cm^{-1} (s, ν(C–H)); 2851.7 cm^{-1} (s, ν(C–H)); 1738.2 cm^{-1} (s, ν(C═O));

1726.4 cm^{-1} (s, ν(C═O)); 1518.4 cm^{-1} (w, ν(O═C–N)); 1441.8 cm^{-1} (s, δ(C–H)); 1406.3 cm^{-1} (s, δ(C–H)); 1366.2 cm^{-1} (m, $\delta_s(CH_3)$); 1201.4 cm^{-1} (s,ν(C–O)); 721.0 cm^{-1} (w, CH_2-rocking).

ω-Mercaptocarboxylic acid linker (Ph_3C-S$(CH_2)_{10}$COOH) (15).[41] 3.00 g (13.80 mmol) 11-mercaptoundecanoic acid was added to a solution of 4.60 g (16.50 mmol) trityl chloride and 4.20 g (33.00 mmol) diisopropylamine in 50 mL of dry toluene. The mixture was stirred under argon for 20 h before the solution was evaporated and resolved in 100 mL of dichloromethane. The solution was washed three times with 100 mL of ethanol and 100 mL of brine solution. The combined organic phases were dried with magnesium sulfate and concentrated *in vacuo*. The product was purified by flash chromatography with silica (cHex–EtOAc, 6 : 1); R_f = 0.16 (cHex–EtOAc, 6 : 1)). Yield: 5.60 g (12.16 mmol, 89%) $C_{30}H_{36}O_2S$ (M = 460.67 g mol^{-1}) [460.24]. ESI-MS (positive), m/z: 483.24 ($[M + Na]^+$, cal.: 483.23), 499.22 ($[M + K]^+$, cal.: 499.20).

^{1}H-NMR (300 MHz, $CDCl_3$), δ (ppm) = 7.41–7.37 (m, 6H, H2ar, H6ar), 7.28–7.23 (m, 6H, H3ar, H5ar), 7.21–7.17 (m, 3H, H4ar), 2.32 (t, 2H, J = 7.4 Hz, CH_2–S), 2.12 (t, 2H, J = 7.3 Hz, CH_2–COOH), 1.63–1.58 (m, 2H, CH_2-CH_2–S), 1.37–1.17 (m, 14H, CH_2).

^{13}C-NMR (75.5 MHz, $CDCl_3$), δ (ppm): 179.5 (COOH), 145.1 (3 × C1ar), 129.7 (3 × C3ar, 3 × C5ar), 127.8 (3 × C2ar, 3 × C6ar), 126.5 (3 × C4ar), 66.3 (S-C-Ph_3), 33.8 (CH_2–COOH), 32.0 (CH_2-S-C-Ph3), 29.3, 29.16, 29.1, 29.0, 28.9, 28.5, 26.9, 24.7 (8 × CH_2).

ω-Mercaptoundecanamido-4,7,10-trioxadodecanylamido-*N*-L-prolyl-L-alanyl-L-histidyl-L-glycyl-L-valyl-*O*-(2-acet-amido-2-deoxy-α-D-galactopyranosyl)-L-threonyl-L-seryl-L-alanyl-L-proline (HS$(C_{10}H_{20})$CONH-$(CH_2CH_2O)_3CH_2CH_2$CONH-Pro-Ala-His-Gly-Val-Thr(αGalNAc)-Ser-Ala-Pro-OH) (GP-03). The glycopeptide **GP-03** was synthesized by the before mentioned standard protocol and modified coupling conditions for the carbohydrate building block **5**. The thiol linker **15** was also coupled under modified conditions together with HATU, HOAt and NMM in NMP using 91.2 mg (0.24 mmol, 2.4 eq.) of compound **15**.

The lyophilisate was dissolved in 1 mL of methanol–toluene (4 : 1) and added slowly into 50 mL cooled Et_2O. The glycopeptide precipitated immediately and was obtained after ultracentrifugation, decantation, redissolvation in water and lyophilization.

Yield: 35.00 mg (0.023 mmol, 23%) colorless lyophilisate.

R_t = 16.14 min (Phenomenex Luna, gradient B see Instrumentation).

ESI-MS (positive), m/z: 1568.89 ($[M + H]^+$, ber.: 1568.78), 784.97 ($[M + 2H]^{2+}$, ber.: 784.89).

^{1}H-NMR (400 MHz, MeOH-d_4, COSY, HSQC), δ (ppm) = 8.54 (d, 1H, JHε,Hδ = 1.02 Hz, Hε), 7.31 (d, 1H, JHδ,Hε = 0.66 Hz, Hδ), 5.12 (d, 1H, JH1,H2 = 3.22 Hz, H1), 4.68–4.17 (m, 10H, Hα {4.65}, Tα {4.60}, A1α {4.52}, Sα {4.45}, P1α {4.40}, 4.33 (dd, 1H, JH2,H1 = 5.24 Hz, JH2,H3 = 12.07 Hz, H2), P2α {4.31}, Tβ {4.27}, Vα {4.22}, A2α {4.20}), 3.82–3.55 (m, 27H, H5 {3.82}, Gαa {3.78}, Gαb {3.76}, H4 {3.74}, H3 {3.64}, H6a,b {3.64}, 3-CH_2-Spacer {3.63}, Sβ {3.62}, 5 × CH_2O-Spacer {3.62}, P1δ {3.60}, P2δ {3.59}, 2-CH_2-Spacer {3.55}, 3.33 (dd, 1H, JHβ,Hα = 5.54 Hz, Hβ), 3.18–3.09 (m, 2H, CH_2-Spacer), 2.91–2.80 (m, 4H, 12-CH_2-Spacer {2.89}, 2-CH_2-Spacer {2.83}), 2.53–2.42 (m, 4H, P1β {2.49}, P2β {2.41}, 2.12, 1.98, 1.97 (s, 9H, 3 × Ac), 2.10–1.90 (m, 9H, Vβ {2.06 }, P1γ {2.04}, P2γ {2.03}, 2 × CH_2-linker {1.91}, 1.37–1.18 (m, 20H, A1β {1.36}, A2β {1.34}, 7 × CH_2-linker {1.29}), 1.21 (d, 3H, JTγ,Hβ = 6.93 Hz, Tγ), 0.97 (t, 6H, JVγ,Vβ = 6.21 Hz, Vγ).

^{13}C-NMR (100.6 MHz, MeOH-d_4, HSQC), δ (ppm) = 172.2, 172.1, 172.1, 172.1, 172.0, 171.9, 171.7, 171.4, 171.2, 171.0, 170.8, 170.5, 170.3, 170.1, 169.9 (C═O, C═O–acetyl), 160.9 (C═NH), 130.5 (Hε), 129.5 (Hγ), 128.4 (Hδ), 99.1 (C1), 77.1 (Tβ), 72.7 (C5), 71.6, 71.4, 71.3, 71.2, 71.1 (CH_2O-Spacer) 70.6 (C4), 69.0 (C3), 67.9 (Sβ), 60.6 (11-CH_2-Spacer), 59.9 (P2α), 59.5 (P1α), 59.2 (Vα), 57.88 (Tα), 56.7 (Sα), 53.8 (Hα), 51.3 (C2), 49.8 (A2α), 49.0, 48.9 (2-CH_2-Spacer), 48.1 (P2δ), 47.6 (A1α), 47.6 (P1δ), 47.5 (C6), 42.4 (Gα), 40.2, 37.1 (12-CH_2-Spacer), 36.0 (CH_2–CO–N-Linker), 31.4 (CH_2-S-C-Ph_3), 31.0 (Vβ), 30.8, 30.6, 30.5, 30.5, 30.4 (5 × CH_2-Linker), 30.3 (P2β), 30.2 (CH_2-Linker), 28.9 (P1β), 28.8 (P2γ), 28.8 (P1γ), 28.5, 28.4 (2 × CH_2-Linker), 27.0 (Hβ), 23.8, 23.2 (2 × CO–CH_3), 22.0 (CH_3–AcNH), 20.7 (CO–CH_3), 19.9 (Tγ), 19.2 (Vγb), 19.1 (Vγa), 16.7 (A2β), 14.7 (A1β).

To remove the carbohydrate protecting groups the glycopeptide was dissolved in 25 mL of methanol and a solution of 0.5 g sodium in 25 mL of methanol was added dropwise until the pH reached 10.5. After stirring for 18 h at room temperature the mixture was neutralized with three drops of concentrated acetic acid, before the solvent was evaporated *in vacuo*. The crude product was purified by a semi-preparative RP-HPLC.

Yield: 20.21 mg (0.0140 mmol, 62.2%) colorless lyophilisate.

R_t = 14.88 min (Phenomenex Luna, gradient B see Instrumentation).

$C_{64}H_{107}N_{13}O_{22}S$ (M = 1442.67 g mol^{-1}) [1441.74].

ESI-MS (positive), m/z: 1442.75 ($[M + H]^+$, ber.: 1442.75), 721.89 ($[M + 2H]^{2+}$, ber.: 721.87), 732.87 ($[M + H + Na]^{2+}$, ber.: 732.87).

Citrate coordinated gold nanoparticles with a diameter of 14 nm (citrate coord. AuNP) (16). A solution of 0.023 g (0.06 mmol) of $HAuCl_4 \cdot 3H_2O$ in 180 mL of water was heated to reflux for 20 min. Under vigorous stirring a solution of 0.101 g (0.34 mmol) of sodium citrate in 1.5 mL of water was added quickly. The reaction mixture was held under reflux for 3 h and then it was cooled to 0 °C in an ice bath. A clear violet solution with a particle concentration of 2.6 nM was obtained and stored at 4 °C. DLS: d_h = 18 ± 4 nm; TEM: d = 14 ± 1 nm; UV/Vis: λ_{max} = 528 nm.

Immobilization of the glycopeptides

GP-01 coordinated gold nanoparticles with a diameter of 7 nm (GP-01 coord. AuNP). GP-01 coordinated gold nanoparticles were obtained by a peptide coupling reaction

of the MUDHSE coordinated AuNP with the glycopeptide **GP-01**.

0.017 g (0.013 mmol) glycopeptide **GP-01** was dissolved in 2 mL of anhydrous DMF, and 1 nmol of MUDHSE coordinated gold nanoparticles solution in 5 mL of anhydrous DMF was added dropwise to the stirring solution. After 30 min 15 μL (0.11 mmol) of triethylamine was added and the solution was stirred at room temperature for another 72 h. Finally the nanoparticle solution was dialysed three times against 400 mL of DMF and 300 mL of triple-distilled water. A red colloid solution with a particle concentration of 0.13 μM was obtained and stored at 4 °C.

DLS: d_h = 17 ± 3 nm; TEM: d = 7 ± 1 nm; UV/Vis: λ_{max} = 524 nm.

^{1}H-NMR (600 MHz, DMSO-d_6, COSY-DQF, HSQC): d = 1.18 (d, 6H, CH_3); 1.25 (d, 3H, CH_3); 1.32–1.41 (m, 12H, CH_2); 1.46 (d, 6H, CH_3); 1.55 (quin, 4H, CH_2); 1.74 (m, 4H, CH_2); 1.98 (m, 1H, CH); 2.01 (m, 4H, CH_2); 2.17 (t, 2H, CH_2); 2.26 (t, 2H, CH_2); 2.45 (m, 1H, CH); 2.55 (t, 2H, CH_2); 2.94 (d, 2H, CH_2); 3.18 (q, 2H, CH_2); 3.38 (t, 2H CH_2); 3.45 (t, 4H, CH_2); 3.50 (bm, 8H, CH_2); 3.65 (t, 2H, CH_2); 3.76 (s, 3H, CH_3); 3.91 (q, 1H, CH); 3.95 (d, 2H, CH_2); 4.12 (d, 1H, CH); 4.15 (t, 2H, CH_2); 4.24 (q, 1H, CH); 4.27 (d, 1H, CH); 4.29 (d, 2H, CH); 4.38 (m, 2H, CH); 4.43–4.48 (m, 4H, CH); 4.51 (m, 2H, CH); 4.72 (d, 1H, CH); 4.92 (bs, 5H, OH); 7.77 (t, 1H, NH); 7.85 (d, 1H, CH); 7.98 (d, 1H, CH); 8.17 (d, 7H, NH); 8.33 (d, 1H, NH) ppm; ATR-IR: 3273.0 cm^{-1} (m; ν(N–H)); 2925.6 cm^{-1} (s; ν(C–H)); 2853.4 cm^{-1} (st; ν(C–H)); 2324.5 cm^{-1} (w); 2164.8 cm^{-1} (w); 1782.6 cm^{-1} (w, ν(C═O)); 1626.1 cm^{-1} (s, ν(C═O)); 1527.1 cm^{-1} (s, ν(C═C)); 1450.8 cm^{-1} (s, δ(C–H)); 1398.8 cm^{-1} (m, δ(C–H)); 1339.4 cm^{-1} (s, δ(C–H)); 1201.2 cm^{-1} (s, ν(C–O)); 1125.3 cm^{-1} (w); 1076.5 cm^{-1} (w); 1044.5 cm^{-1} (w); 718.2 cm^{-1} (w, CH_2-rocking).

GP-02 coordinated gold nanoparticles with a diameter of 7 nm (GP-02 coord. AuNP). A 0.2 μM (1.6 nmol) solution of MUDHSE coordinated AuNP in 8 mL of anhydrous DMF was added dropwise to a solution of 0.036 g (0.016 mmol) **GP-02** in 2 mL anhydrous DMF. After 30 min of stirring at room temperature 15 μL (0.11 mmol) of triethylamine was added and the mixture was stirred for another 24 h. The clear colloid solution was dialyzed three times against 600 mL DMF and 600 mL of triple-distilled water. For storage the colloid solution was diluted to a 0.32 μM concentration of nanoparticles.

DLS: d_h = 34 ± 7 nm; TEM: d = 7 ± 1 nm; UV/Vis: λ_{max} = 524 nm.

GP-03 coordinated gold nanoparticles with a diameter of 14 nm (GP-03 coord. AuNP). A solution of 0.015 g (0.01 mmol) **GP-03** in 3 mL of triple-distilled water was added to 20 mL of a 1.72 μM aqueous solution of Au/citrate and the mixture was stirred for 72 h. Then the particles were dialysed three times against 600 mL of triple-distilled water. After concentration of the solution to 10 mL a 3.4 nM particle solution was obtained and stored at 4 °C.

DLS: d_h = 19 ± 4 nm; TEM: d = 14 ± 1 nm; UV/Vis: λ_{max} = 531 nm.

Acknowledgements

The authors thank Timo Schueler for the QCM measurements.

References

1 (*a*) J. N. Blattman and P. D. Greenberg, *Science*, 2004, **305**, 200; (*b*) C. J. Melief and S. H. van der Burg, *Nat. Rev. Cancer*, 2008, **8**, 351.
2 (*a*) J. A. Berzofsky, M. Terabe, S. Oh, I. M. Belyakov, J. D. Ahlers, J. E. Janik and J. C. Morris, *J. Clin. Invest.*, 2004, **113**, 1515–1525; (*b*) I. Espinoza-Delgado, *Oncologist*, 2002, **7**(Suppl 3), 20; (*c*) E. Jager, D. Jager and A. Knuth, *Int. J. Cancer*, 2003, **106**, 817–820.
3 M. S. Mitchell, *Int. J. Immunopharmacol.*, 2003, **3**, 1051.
4 Y. Krishnamachari, S. M. Geary, C. D. Lemke and A. K. Salem, *Pharm. Res.*, 2011, **28**, 215–236.
5 (*a*) P. E. Constantinou, B. P. Danysh, N. Dharmaraj and D. D. Carson, *Expert Rev. Endocrinol. Metab.*, 2011, **6**, 835; (*b*) A. Hoffmann-Röder, A. Kaiser, S. Wagner, N. Gaidzik, D. Kowalczyk, U. Westerlind, B. Gerlitzki, E. Schmitt and H. Kunz, *Angew. Chem., Int. Ed.*, 2010, **122**, 1; (*c*) T. Renno, S. Lebecque, N. Renard, S. Saeland and A. Vicari, *Cell. Mol. Life Sci.*, 2003, **60**, 1296; (*d*) M. L. Disis, K. H. Grabstein, P. R. Sleath and M. A. Cheever, *Clin. Cancer Res.*, 1999, **5**, 1289.
6 (*a*) J. R. Gum Jr., *Biochem. Soc. Trans.*, 1995, **23**, 795; (*b*) I. Carlsted and J. R. Davies, *Biochem. Soc. Trans.*, 1997, **25**, 214; (*c*) A. Girling, J. Bartkova, J. Burchell, S. Gendler, C. Gillet and J. Taylor-Papadimiriou, *Int. J. Cancer*, 1989, **43**, 1072; (*d*) M. A. Tarp and H. Clausen, *Biochim. Biophys. Acta Gen. Subj.*, 2008, **1780**, 546.
7 (*a*) U. Westerlind, H. Schröder, A. Hobel, N. Gaidzik, A. Kaiser, C. M. Niemeyer, E. Schmitt, H. Waldmann and H. Kunz, *Angew. Chem., Int. Ed.*, 2009, **48**, 8263; (*b*) F. Carzana, J. M. Busto, F. Marcelo, M. G. de Luis, J. C. Abensio, S. Martín-Santamaría, J. Jiménez-Barbero, A. Avenoza and J. M. Peregrina, *Chem. – Eur. J.*, 2011, **17**, 3105.
8 (*a*) A. Kaiser, N. Gaidzik, U. Westerlind, D. Kowalczyk, A. Hobel, E. Schmitt and H. Kunz, *Angew. Chem., Int. Ed.*, 2009, **121**, 7688; (*b*) D. H. Dube and C. R. Bertozzi, *Nat. Rev. Drug Discovery*, 2005, **4**, 477.
9 (*a*) N. Gaidzik, U. Westerlind and H. Kunz, *Chem. Soc. Rev.*, 2013, **42**, 4421; (*b*) T. Buskas, P. Thompson and G. J. Boons, *Chem. Commun.*, 2009, 5335; (*c*) R. D. Astronomo and D. R. Burton, *Nat. Rev. Drug Discovery*, 2009, **9**, 308; (*d*) S. F. Slovin, S. J. Keding and G. Ragupathi, *Immunol. Cell Biol.*, 2005, **83**, 418; (*e*) R. E. Beatson, J. Taylor-Papadimitriou and J. M. Burchell, *Immunotherapy*, 2010, **2**, 305; (*f*) S. H. Itzkowitz, M. Yuan, C. K. Montgomery, T. Kjeldsen, H. K. Takahashi, W. L. Bigbee and Y. S. Kim, *Cancer Res.*, 1989, **49**, 197–204.
10 Y. S. Kim, J. Gum Jr. and I. Brockhausen, *Glycoconjugate. J.*, 1996, **13**, 693.

11 F. Berti and R. Adamo, *Chem. Biol.*, 2013, **8**, 1653.
12 (*a*) S. J. Danishefsky and J. A. Allen, *Angew. Chem., Int. Ed.*, 2000, **112**, 882; (*b*) G. D. MacLean, M. A. Reddish, R. R. Koganty and B. M. Longenecker, *J. Immunother.*, 1996, **19**, 59; (*c*) B. M. Longenecker, M. Reddish, R. Koganty and G. D. MacLean, *Adv. Exp. Med. Biol.*, 1994, **353**, 105; (*d*) N. Gaidzik, A. Kaiser, D. Kowalczyk, U. Westerlind, B. Gerlitzki, H. P. Sinn, E. Schmitt and H. Kunz, *Angew. Chem., Int. Ed.*, 2011, **123**, 10153; (*e*) T. Nolan, S. Lambert, D. Roberton, H. Marshall, P. Richmond, C. Streeton, J. Poolman and D. Boutriau, *Vaccine*, 2007, **25**, 8487.
13 P. Spohn, U. Buwitt-Beckmann, R. Bock, G. Jung, A. J. Ulmer and K.-H. Wiesmueller, *Vaccine*, 2004, **22**, 2494.
14 A. Hoffmann-Roeder and M. Johannes, *Chem. Commun.*, 2011, **47**, 9903.
15 O. Renaudet and P. Dumy, *Org. Lett.*, 2003, **5**, 243.
16 S. Keil, A. Kaiser, F. Syed and H. Kunz, *Synthesis*, 2009, 1355.
17 S. Ingale, T. Buskas and G.-J. Boons, *Org. Lett.*, 2006, **8**, 5785.
18 (*a*) J. M. de la Fuente and S. Penadés, *Biochim. Biophys. Acta*, 2006, **1760**, 636; (*b*) R. P. Brinas, A. Sundgren, P. Sahoo, S. Morey, K. Rittenhouse-Olson, G. E. Wilding, W. Deng and J. J. Barchi Jr., *Bioconjugate Chem.*, 2012, **23**, 1513; (*c*) B. P. Danysh, P. E. Constantinou, E. Y. Lukianova-Hleb, D. O. Lapotko and D. D. Carson, *Theranostics*, 2012, **2**, 777; (*d*) R. Savla, O. Taratula, O. Garbuzenko and T. Minko, *J. Controlled Release*, 2011, **153**, 16; (*e*) E. S. Glazer, C. Zhu, K. L. Massey, C. S. Thompson, W. D. Kaluarachchi and A. N. Hamir, *Clin. Cancer Res.*, 2010, **16**, 5712.
19 (*a*) G. B. Sigal, M. Mammen, G. Dahmann and G. M. Whitesides, *J. Am. Chem. Soc.*, 1996, **118**, 3789; (*b*) M. Mammen, S.-K. Choi and G. M. Whitesides, *Angew. Chem.*, 1998, **110**, 2908.
20 (*a*) J. Dernedde, S. Enders, H.-U. Reissig, M. Roskamp, S. Schlecht and S. Yekta, *Chem. Commun.*, 2009, **8**, 932; (*b*) M. Roskamp, S. Enders, F. Pfrengle, S. Yekta, V. Dekaris, J. Dernedde, H.-U. Reissig and S. Schlecht, *Org. Biomol. Chem.*, 2011, **9**, 7448.
21 (*a*) C. M. Niemeyer, *Angew. Chem., Int. Ed.*, 2001, **113**, 4254; (*b*) C. Buzea, I. I. Pacheco and K. Robbie, *Biointerphases*, 2007, **4**, 17; (*c*) C. M. Niemeyer, *Angew. Chem., Int. Ed.*, 2001, **40**, 4128; (*d*) R. Ojeda, J. L. de Paz, A. G. Barrientos, M. M. Lomas and S. Penadés, *Carbohydr. Res.*, 2007, **342**, 448; (*e*) A. Sundgren and J. J. Barchi Jr., *Carbohydr. Res.*, 2008, **343**, 1594.
22 L. Nuhn, S. Hartmann, B. Palitzsch, B. Gerlitzki, E. Schmitt, R. Zentel and H. Kunz, *Angew. Chem., Int. Ed.*, 2013, **52**, 10652.
23 M. C. Daniel and D. Astruc, *Chem. Rev.*, 2004, **104**, 293.
24 A. Kaiser, N. Gaidzik, U. Westerlind, D. Kowakczyk, A. Hobel, E. Schmitt and H. Kunz, *Angew. Chem., Int. Ed.*, 2009, **48**, 7551.
25 H. Paulsen and K. Adermann, *Liebigs Ann. Chem.*, 1989, 751.
26 (*a*) H. Paulsen and J. P. Hoelck, *Carbohydr. Res.*, 1982, **109**, 89; (*b*) W. Koenigs and E. Knorr, *Chem. Ber.*, 1901, **34**, 957.
27 E. Meinjohanns, M. Meldal, A. Schleyer, H. Paulsen and K. Bock, *J. Chem. Soc., Perkin Trans. 1*, 1996, 985.
28 (*a*) D. Stucky, *et al.*, *J. Am. Chem. Soc.*, 2006, **128**, 6550; (*b*) J. Turkevich, P. C. Stevenson and J. Hillier, *Discuss. Faraday Soc.*, 1951, **11**, 55; (*c*) J. Turkevich, *Gold Bull.*, 1985, **18**, 86; (*d*) G. Frens, *Nat. Phys. Sci.*, 1973, **241**, 20.
29 E. Oh, K. Susumu, A. J. Makinen, J. R. Deschamps, A. L. Huston and I. L. Medintz, *J. Phys. Chem. C*, 2013, **117**, 18947.
30 B. C. Mei, E. Oh, K. Susumu, D. Farrell, T. J. Mountziaris and H. Mattoussi, *Langmuir*, 2009, **25**, 10604.
31 A. Dass, R. Guo, J. B. Tracy, R. Balasubramanian, A. D. Douglas and R. W. Murray, *Langmuir*, 2008, **24**, 310.
32 K. B. Cederquistm and C. D. Keating, *Nano*, 2009, **3**, 256.
33 T. Platen, T. Schueler, W. Tremel and A. Hoffmann-Roeder, *Eur. J. Org. Chem.*, 2011, 3878.
34 (*a*) J. Burchell, S. Gendler, J. Taylor-Papadimitriou, A. Girling, A. Lewis, R. Millis and D. Lamport, *Cancer Res.*, 1987, **47**, 5476–5482; (*b*) J. Burchell, J. Taylorpapadimitriou, M. Boshell, S. Gendler and T. Duhig, *Int. J. Cancer*, 1989, **44**, 691–696.
35 H. Moeller, N. Serttas, H. Paulsen, J. M. Burchell, J. Taylor-Papadimitriou and B. Meyer, *Eur. J. Biochem.*, 2002, **269**, 1444.
36 R. U. Lemieux and R. M. Ratcliffe, *Can. J. Chem.*, 1979, **57**, 1244.
37 A. Paquet, *Can. J. Chem.*, 1982, **60**, 976.
38 B. Liebe and H. Kunz, *Helv. Chim. Acta*, 1997, **80**, 1473.
39 S. Keil, C. Claus, W. Dippold and H. Kunz, *Angew. Chem.*, 2001, **113**, 379.
40 O. Seitz and H. Kunz, *J. Org. Chem.*, 1997, **62**, 813.
41 D. Liu, H. Shao and X. Jiang, *Angew. Chem., Int. Ed.*, 2009, **48**, 4406.